WAVE PROPAGATION IN A CIRCULAR MEMBRANE SUBJECTED TO AN IMPULSIVELY APPLIED PRESSURE LOAD

by

David Vernon Hutton

Thesis submitted to the Graduate Faculty of the
Virginia Polytechnic Institute and State University
in partial fulfillment of the requirements for the degree of

MASTER OF SCIENCE

in

Engineering Mechanics

APPROVED:

J. Counts, Chairman

F. J. Maher

K. L. Reifsnider

February, 1972

Blacksburg, Virginia

ACKNOWLEDGMENTS

The author wishes to express his appreciation to Professor J. Counts of the Engineering Mechanics Department, Virginia Polytechnic Institute and State University, for all the guidance and helpful criticisms given during the course of this study. The author also expresses his gratitude for the patience and encouragement of his wife during the long hours of this investigation.

TABLE OF CONTENTS

	Page
ACKNOWLEDGMENTS	ii
LIST OF FIGURES	v
LIST OF TABLES	vii
LIST OF APPENDICES	viii
LIST OF SYMBOLS	ix
I. INTRODUCTION	1
II. REVIEW OF PERTINENT LITERATURE	3
III. ANALYSIS OF THE GOVERNING EQUATIONS	9
General Problem	9
Equations of Motion	9
The Constitutive Relation	14
Classification of the Equations of Motion	15
Numerical Procedure	18
Alternate Numerical Procedure	23
Linearly Elastic Action	28
Initial Conditions	29
IV. RESULTS	30
Physical Parameters	30
Numerical Convergence Data	32
Propagation of the Strain Wave	33
Propagation of the Inertia Wave	42
Radial Velocity	49

TABLE OF CONTENTS - continued

Page

Effect of Pressure Magnitude on Yield Point 51

Axial Deflection 54

V. CONCLUDING REMARKS 57

VI. LIST OF REFERENCES 60

APPENDIX A 61

VITA 77

ABSTRACT

LIST OF FIGURES

		Page
1.	Membrane mechanism of Hudson and Frederick	4
2.	Deflection profiles of Frederick	6
3.	Element of the membrane and force system to which it is subjected	10
4.	Meridian line of the membrane	12
5.	Main characteristic mesh	20
6.	Interior loop of the characteristic network	21
7.	Characteristic mesh at the boundaries	24
8.	Meridional stress distribution illustrating convergence. .	34
9.	Alternate convergence data--meridional stress history at r/R = 0.9	35
10.	Leading C_{II}^{-} characteristic	37
11.	Meridional stress distribution at succeeding times	38
12.	Meridional stress distribution at succeeding times	40
13.	Meridional stress distribution at succeeding times	41
14.	Position of slope discontinuity as a function of time . .	44
15.	Axial velocity distribution at t = 20 microseconds	45
16.	Axial velocity distribution at t = 25 microseconds	46
17.	Axial velocity distribution at t = 28 microseconds	47
18.	Axial velocity of center of the membrane as a function of time	48
19.	Axial velocity at r/R = 0.95 as a function of time	50
20.	Radial velocity distribution at yield	52

LIST OF FIGURES - continued

Page

21. Meridional stress distribution at succeeding times for increased loading 53

22. Successive membrane profiles for a hypothetical elastic material 56

LIST OF TABLES

		Page
1.	Some possible pressure-radius-thickness combinations corresponding to p_o = 20,000 psi	31

LIST OF APPENDICES

		Page
A.	Listing of Fortran programs used to obtain numerical results	61

LIST OF SYMBOLS

C_I	Velocity of propagation of the inertia waves
C_{II}	Velocity of propagation of the strain waves
$\vec{e}_1$	Unit vector in the radial direction
$\vec{e}_2$	Unit vector in the vertical direction
$\vec{e}_N$	Unit vector normal to the membrane
$\vec{e}_T$	Unit vector tangential to the membrane
E	Modulus of elasticity
F, F_1, F_2	Functions defined by equations (17)
h	Thickness of the membrane
h_o	Initial thickness of the membrane
msec	Milliseconds
P	Applied pressure
P_o	Maximum value of applied pressure
p	Scaled value of applied pressure
p_o	Maximum value of scaled pressure
R	Radius of the membrane
R_c	Radius of curvature
$R_{11}, R_{12}, R_{21}, R_{22}, R_3$	Force components defined by equations (1)
$\vec{R}$	Position vector of a point on the membrane
r	Actual radial coordinate
r_o	Initial radial coordinate

s	Arc length along the membrane
t	Dimensional time
T_o	Initial tension
$\vec{v}$	Velocity of a point on the membrane
w	Axial deflection
ξ	Non-dimensional thickness
$\varepsilon_1, \varepsilon_2, \varepsilon_3$	Meridional, circumferential and normal strain, respectively
μsec	Microseconds
η	Non-dimensional radial coordinate
η_o	Non-dimensional initial radial coordinate
ρ	Actual density of membrane material
ρ_o	Initial density of membrane material
Φ_1, Φ_2, Φ_3	Angles defined in Figure 4
$\sigma_1, \sigma_2, \sigma_3$	Meridional, circumferential and normal stress components, respectively
ψ	Non-dimensional arc length
τ	Non-dimensional time
ν	Poisson's ratio
ω	Non-dimensional axial deflection

Subscripts

η_o	Differentiation with respect to η_o
τ	Differentiation with respect to τ
ψ	Differentiation with respect to ψ

I. INTRODUCTION

The study of the mechanics of circular membranes has various technological applications. In the chemical process industry, for example, thin metal discs, called rupture discs, are used to protect process vessels from deformation or failure due to internal over-pressure. In this application, the discs are installed in a vent line from the vessel, and, as the vessel pressure increases, the disc bulges and finally ruptures, thus providing a vent for pressure release. The pressure at which rupture occurs is based upon the safe working limits of the vessel, and, as is known from personal experience, manufacturers of rupture discs rely heavily upon destructive testing to determine rupture pressures.

In the case of axial symmetry, the circular membrane problem is formulated in terms of a single spatial variable, the radial coordinate. In this sense, the problem then becomes a one dimensional problem. The equations of motion, written in the radial and vertical directions, are a pair of second-order, non-linear, partial differential equations which are coupled in first derivatives. Both circumferential and meridional stress components appear in the equations; thus, the equations are complicated to such an extent that a closed-form solution appears to be all but impossible to obtain.

This problem has been studied experimentally by various authors, but the analytic approach appears to have received limited attention. Generally, the analytic solutions that have been obtained are based on various simplifying assumptions which are discussed later.

The objective of this work is to obtain a numerical solution to the problem of a circular membrane subjected to an impulsively applied pressure of constant magnitude, distributed uniformly across the membrane. The governing equations are derived and are classified as completely hyperbolic. The solution is obtained using the method of characteristics and finite difference techniques on a digital computer. The membrane material is considered to obey a linearly elastic constitutive relation and is isotropic and homogeneous. This study is intended to be preliminary to the investigation of similar problems in plasticity and composite materials.

II. REVIEW OF PERTINENT LITERATURE

The dynamic deformation of a membrane is a problem area which has received limited theoretical analysis. Due to the presence of a two-dimensional state of stress, the complete equations of motion are quite complex. However, various authors have considered the problem under the assumptions of perfectly plastic material behavior and neglecting the elastic phase of the deformation. Under these assumptions, the equations of motion are considerably simplified and solutions have been obtained.

G. E. Hudson [1] considered the case of a circular membrane clamped at the periphery and given a uniform velocity in the axial direction. Elastic effects were neglected by assuming that the initial elastic wave has infinite speed and that the stress jumps from zero to the yield stress. The material behavior was then considered to be that of an ideal incompressible plastic material. The assumed mode of deformation of the membrane is shown in Figure 1. A hinge developed at the boundary and moved inward toward the center. The movement of the hinge separates the membrane into two regions: an outer region which is assumed rigid and conical; and a flat circular region which moves upward with constant velocity and decreases in size. Once the hinge reaches the center it is assumed to remain there, and the membrane becomes conical in shape.

D. Frederick [2] considered the problem in a manner similar to Hudson. Frederick investigated the deformation of a circular membrane for the cases of both ideal plasticity and work hardening, and compared the theoretical deformations to those obtained experimentally by subjecting steel plates to underwater explosions. Some of the results are

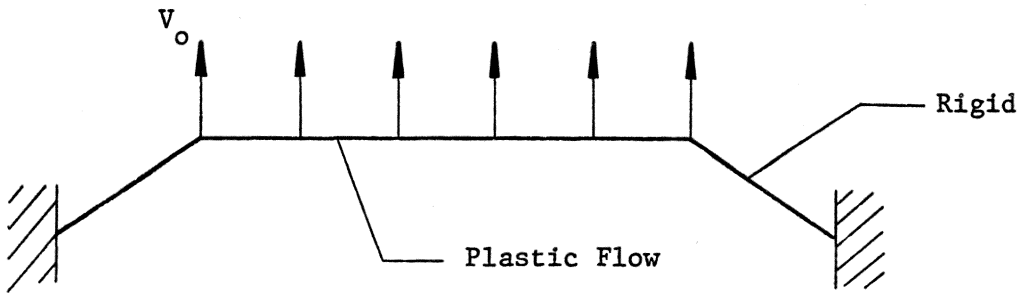

Figure 1. Membrane mechanism of Hudson and Frederick.

shown in Figure 2. The theoretical profile is conical as in Hudson's analysis, and the deflections calculated for ideal plasticity are seen to be somewhat lower than the experimental value. This discrepancy is due in part to the assumption of rigidity in the outer section and neglecting the elastic deformations. It is also seen that the deflections calculated using work-hardening are in poorer agreement with experiment than those for the ideal material.

G. Munday and D. M. Newitt [3] studied the deformation of a circular membrane subjected to a transverse pressure loading. The complete equations of motion for the membrane were derived as were the equations for the deflection of an extensible wire under similar conditions. Munday and Newitt concluded that the equations for the wire are hyperbolic differential equations which can be solved by the method of characteristics. The conclusion for the membrane, however, was that the inclusion of the circumferential stress precludes any characteristic solution. As will be shown in this study, the membrane equations are also hyperbolic and may in fact be solved numerically by the method of characteristics.

By assuming the change in membrane thickness to be negligible and that the stress throughout the membrane was equal to the yield stress, Munday and Newitt simplified the equation of motion in the transverse direction to a form such that a solution for the vertical deflection could be found using the method of Laplace transforms. In order to verify the solution, experiments were performed using copper discs with the loading exerted by a shock tube. The deflections of the discs were observed and measured using high speed photography. The mechanism of

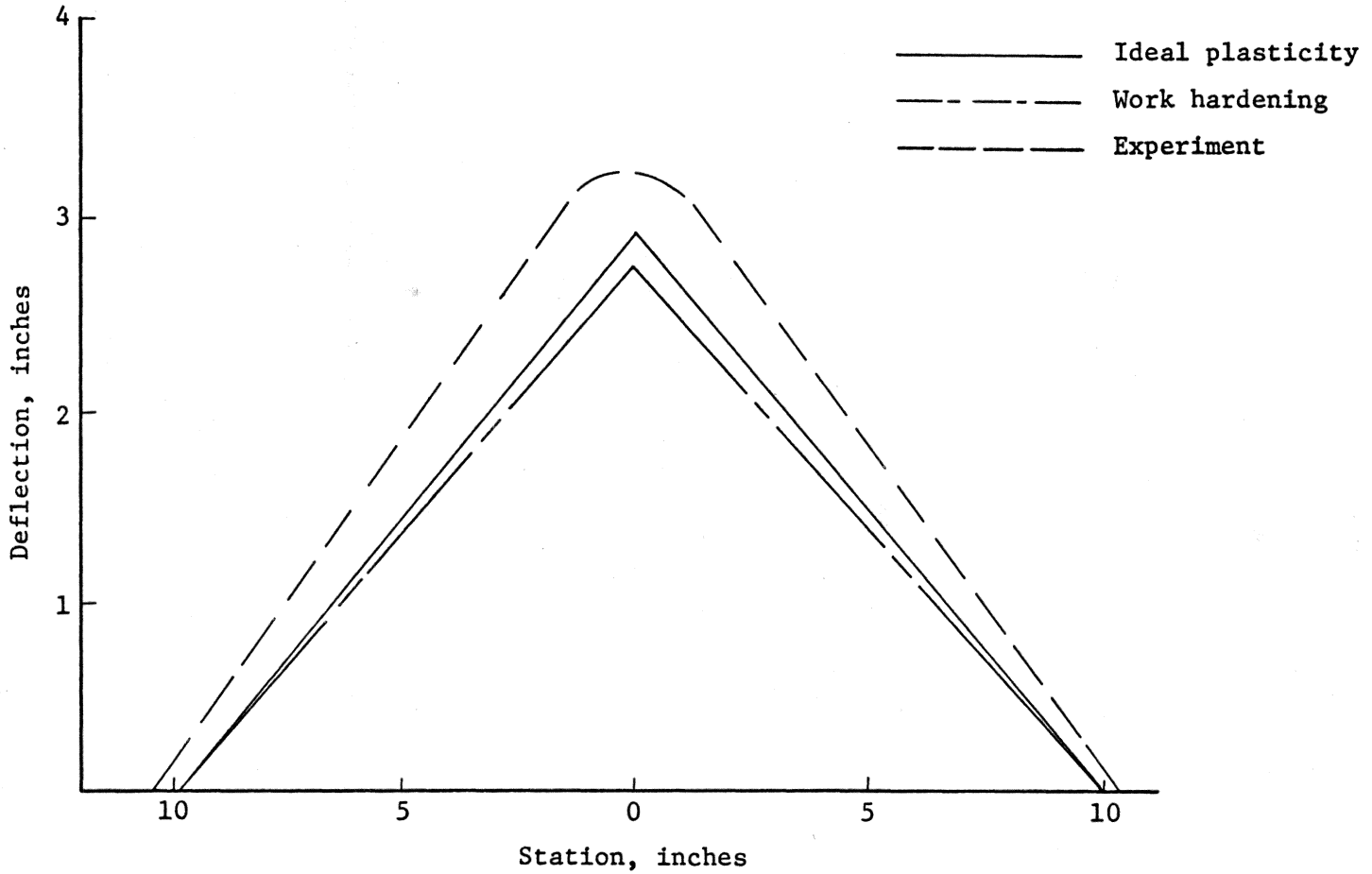

Figure 2. Deflection profiles of Frederick.

deformation was seen to agree with that of Hudson and Frederick, and the shape of the disc in its final deformed position was found to be in good agreement with the theoretical solution at the instant when the hinge reaches the center.

Probably the most extensive treatment of the mechanics of circular membranes is that given by N. Cristescu [4]. Various technological applications are discussed, and a fairly complete review of the literature is presented. In examining the mathematics of the problem, Cristescu first considered the case in which the circumferential stress is neglected in order to find some indication of the phenomena involved. The equations of motion are formulated, assuming a finite constitutive equation, and found to be hyperbolic partial differential equations possessing four families of characteristics. A procedure for numerical solution using the method of characteristics is outlined but no results given as the formulation is not specialized to a particular loading or constitutive equation.

Cristescu has also examined the more general case taking into account the circumferential stress. The membrane is considered to deform under the action of an axially symmetric transverse pressure which may vary with both time and position. The analysis is given for both finite and differential constitutive equations, and it is shown that the equations for both cases may be solved numerically, in theory, by the method of characteristics. For the case of a finite constitutive equation, four families of characteristics exist representing the propagation of both transverse and longitudinal waves in the membrane. A detailed procedure for numerical integration along the characteristic

lines is given, and initial and boundary conditions are discussed for several example problems. A similar analysis is given for a differential constitutive equation except that no numerical procedure is presented. Again for the general case, no numerical results are presented as the analyses are completely general in regard to loading and constitutive relation.

Related studies have been performed on the deformation of membranes having geometries other than circular. F. J. Kay and G. D. Whitehouse [5] have obtained a solution for the plastic deformation of a clamped rectangular membrane subjected to an impulsive load. A hinge concept similar to that of Hudson and Frederick is used. The shape of the hinge line is assumed to be a hyper-ellipse. This hyper-elliptic formulation embodies the assumption that the hinge develops at the boundary and is also consistent with the experimental evidence that deformation deep into the corners does not occur. By reducing the rectangular solution to that for a circular membrane, the results were shown to be in agreement with those of both Hudson and Frederick. B. Karunes and E. T. Onat [6] considered the case of a rectangular membrane attached to two parallel fixed supports. The deformation is due to an impulsive velocity distributed uniformly across the membrane. In any plane normal to the supports a cross section through the membrane will move like an extensible string. The analysis is presented using the analogy with strings for a material which is plastic/rigid and linear strain-hardening.

III. ANALYSIS OF THE GOVERNING EQUATIONS

General Problem

The membrane is initially planar and at t = 0 lies in the r - θ plane of a cylindrical coordinate system. The periphery of the membrane is rigidly clamped. The loading is considered to be axisymmetric but may be a function of radial position and/or time. It is assumed that body forces acting on the membrane are small in comparison to the applied loading and are neglected.

Equations of Motion

The equations of motion are written in reference to the element of the membrane depicted in Figure 3. A system of cylindrical coordinates is used, with the origin taken at the center of the membrane. The initial, or Lagrangian, coordinate is r_o, while r is the actual coordinate. The vertical axis is taken positive downward so that $\partial r/\partial s$ and the radius of curvature are positive.

The meridional and circumferential directions will be denoted by the subscripts 1 and 2, respectively. Thus, the meridional and circumferential stresses are σ_1 and σ_2, respectively. The third stress component, σ_3, is normal to the membrane and is neglected because the membrane thickness is small in comparison to the radius.

The forces which act on the element are

$$R_{11} = \sigma_1 hrd\theta \qquad R_{12} = (\sigma_1 + d\sigma_1)(h + dh)(r + dr)\, d\theta$$

$$R_{21} = R_{22} = \sigma_2 hds \qquad R_3 = Prd\theta ds \tag{1}$$

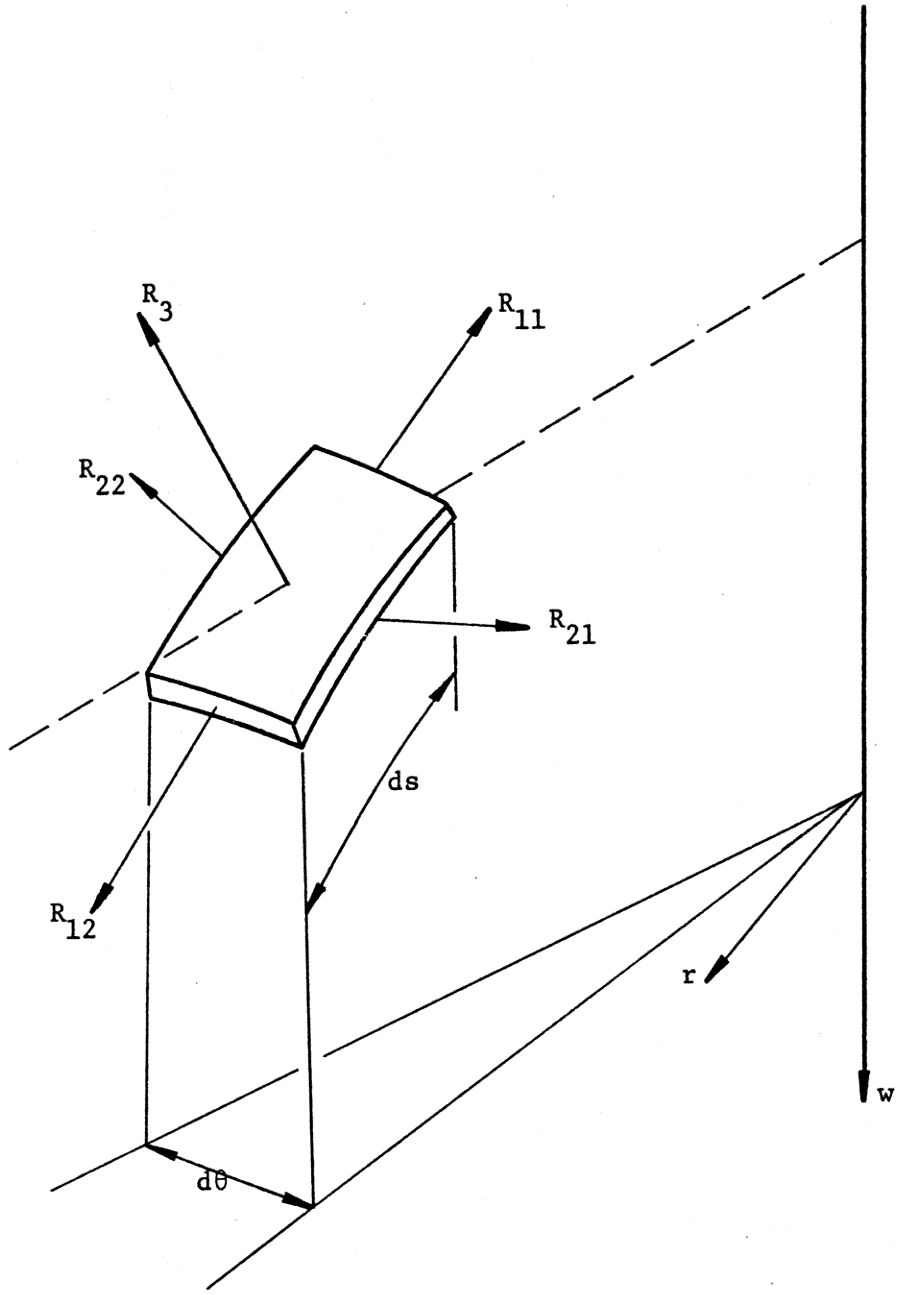

Figure 3. Element of the membrane and force system to which it is subjected.

where h is the thickness of the element and s is the arc length of the element in the meridional direction.

Due to axial symmetry, there is no motion in the circumferential direction, and the equations of motion may now be written with reference to Figure 4. The angles used to write the equations are

$$\sin\Phi_3 = \cos\Phi_1 = \frac{\partial r}{\partial s} \qquad \cos\Phi_3 = \sin\Phi_1 = \frac{\partial w}{\partial s}$$
$$\cos\Phi_2 = \frac{\partial r}{\partial s} - \frac{\partial w}{\partial s}\frac{ds}{R_c} \qquad \sin\Phi_2 = \frac{\partial w}{\partial s} + \frac{\partial r}{\partial s}\frac{ds}{R_c} \tag{2}$$

where R_c is the radius of curvature, given by

$$R_c = \frac{\left[1 + \left(\frac{\partial w}{\partial s}\right)^2\right]^{3/2}}{\frac{\partial^2 w}{\partial r^2}} \quad , \tag{3}$$

and w is the deflection in the vertical direction.

Writing Newton's second law in the radial and vertical directions and neglecting higher order terms, the equations of motion are

$$hr\,\rho\frac{\partial^2 r}{\partial t^2} = Pr\,\frac{\partial w}{\partial s} + \frac{\partial}{\partial s}\left(\sigma_1 hr\frac{\partial r}{\partial s}\right) - \sigma_2 h$$
$$hr\,\rho\frac{\partial^2 w}{\partial t^2} = -\,Pr\,\frac{\partial r}{\partial s} + \frac{\partial}{\partial s}\left(\sigma_1 hr\frac{\partial w}{\partial s}\right) \quad , \tag{4}$$

and the continuity equation is

$$rh\rho = r_o h_o \rho_o \frac{dr_o}{ds} \quad , \tag{5}$$

where h_o is the initial thickness of the membrane, ρ and ρ_o are the actual and initial densities, and $P = P(r,t)$ is the applied pressure.

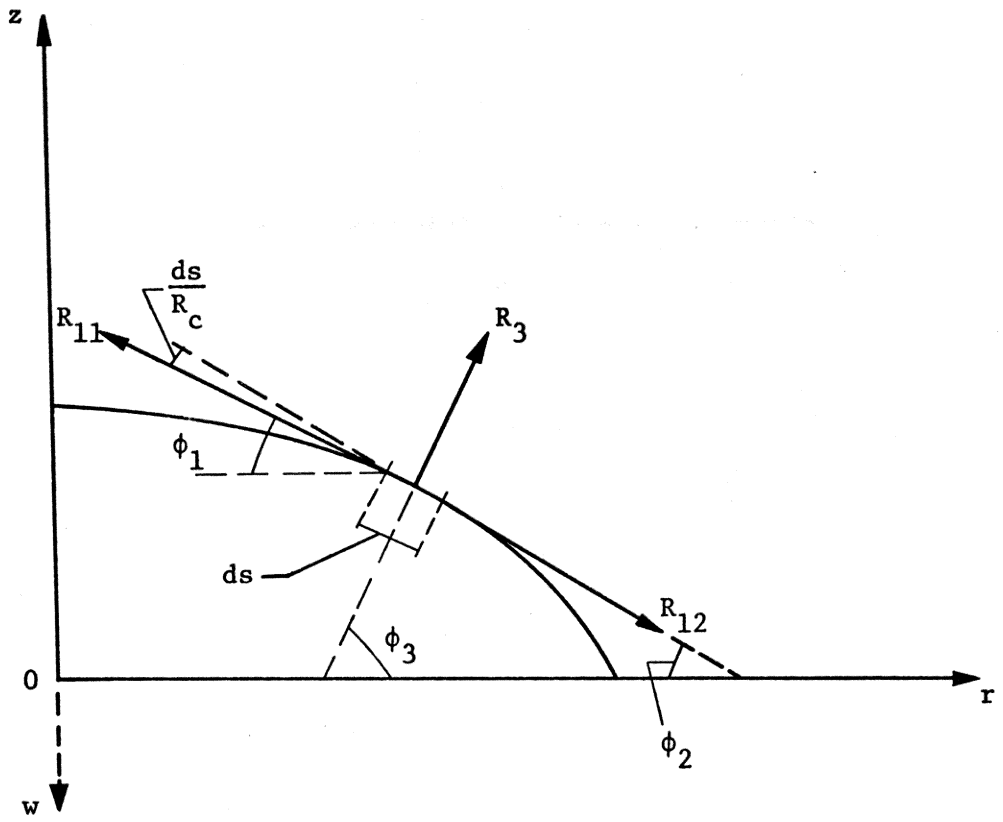

Figure 4. Meridian line of the membrane.

Denoting the radius of the membrane by R and the maximum value of $P(r,t)$ by P_o, the equations of motion are made non-dimensional by introducing

$$\eta = \frac{r}{R}, \quad \omega = \frac{w}{R}, \quad \xi = \frac{h}{h_o}, \quad \tau = \left[\frac{P_o}{Rh_o\rho_o}\right]^{1/2} t,$$
$$\eta_o = \frac{r_o}{R}, \quad \psi = \frac{s}{R}, \quad p_o = \frac{P_o R}{h_o}, \quad p = \frac{PR}{h_o} . \tag{6}$$

Substituting these variables, equations (4) become

$$\xi\eta\frac{\rho}{\rho_o}\frac{\partial^2\eta}{\partial\tau^2} = \frac{p}{p_o}\eta\frac{\partial\omega}{\partial\psi} + \frac{\partial}{\partial\psi}\left(\xi\eta\frac{\sigma_1}{p_o}\frac{\partial\eta}{\partial\psi}\right) - \frac{\sigma_2}{p_o}\xi$$
$$-\xi\eta\frac{\rho}{\rho_o}\frac{\partial^2\omega}{\partial\tau^2} = \frac{p}{p_o}\eta\frac{\partial\eta}{\partial\psi} - \frac{\partial}{\partial\psi}\left(\xi\eta\frac{\sigma_1}{p_o}\frac{\partial\omega}{\partial\psi}\right) \tag{7}$$

and equation (5) is

$$\xi\eta\rho\frac{d\psi}{d\eta_o} = \eta_o\rho_o . \tag{8}$$

If we set $\rho = \rho_o$, the equations are identical to those obtained by Munday and Newitt [3].

In order to write the equations of motion in terms of the Lagrangian coordinate η_o, the strain components

$$\varepsilon_1 = \frac{d\psi - d\eta_o}{d\eta_o} = \sqrt{\left(\frac{\partial\eta}{\partial\eta_o}\right)^2 + \left(\frac{\partial\omega}{\partial\eta_o}\right)^2} - 1$$
$$\varepsilon_2 = \frac{\eta d\theta - \eta_o d\theta}{\eta_o} = \frac{\eta}{\eta_o} - 1 \tag{9}$$
$$\varepsilon_3 = \frac{h}{h_o} - 1 = \xi - 1$$

will be introduced. Using the definition of the strain components together with equation (8), the equations of motion can now be written

$$\eta_o \frac{\partial^2 \eta}{\partial \tau^2} = \frac{p}{p_o} \eta \frac{\partial \omega}{\partial \eta_o} + \frac{\partial}{\partial \eta_o}\left(\frac{\xi \eta}{1+\varepsilon_1} \frac{\sigma_1}{p_o} \frac{\partial \eta}{\partial \eta_o}\right) - (1+\varepsilon_1) \frac{\sigma_2}{p_o} \xi$$

$$-\eta_o \frac{\partial^2 \omega}{\partial \eta^2} = \frac{p}{p_o} \eta \frac{\partial \eta}{\partial \eta_o} - \frac{\partial}{\partial \eta_o}\left(\frac{\xi \eta}{1+\varepsilon_1} \frac{\sigma_1}{p_o} \frac{\partial \omega}{\partial \eta_o}\right) . \tag{10}$$

Equations (1) are identical to those obtained by Cristescu [4] as equations (4.8), page 316, and by Cristescu and I. Suliciu [11] as equations 2.8, page 46.

The Constitutive Relation

If we consider a finite constitutive equation, we may write

$$\sigma_1 = \sigma_1(\varepsilon_1, \varepsilon_2, \varepsilon_3)$$

$$\sigma_2 = \sigma_2(\varepsilon_1, \varepsilon_2, \varepsilon_3) \tag{11}$$

$$\sigma_3 = \sigma_3(\varepsilon_1, \varepsilon_2, \varepsilon_3) = 0.$$

Then from the last of equations (11), it follows that the constitutive equations may be written

$$\sigma_1 = \sigma_1(\varepsilon_1, \varepsilon_2)$$

$$\sigma_2 = \sigma_2(\varepsilon_1, \varepsilon_2) , \tag{12}$$

and the parameter ξ is

$$\xi = 1+\varepsilon_3 = g(\varepsilon_1, \varepsilon_2) .$$

Classification of the Equations of Motion

Chou and Perry [7] have shown that a system of two second order, quasi-linear, partial differential equations

$$\begin{aligned} A_1 u_1'' + B_1 u_2'' + C_1 \ddot{u}_1 + D_1 \ddot{u}_2 + E_1 \dot{u}_1' + F_1 \dot{u}_2' &= R_1 \\ A_2 u_2'' + B_2 u_2 + C_2 \ddot{u}_1 + D_2 \ddot{u}_2 + E_2 \dot{u}_1' + F_2 \dot{u}_2' &= R_2, \end{aligned} \tag{14}$$

where $u_i = u_i(x,t)$, may be classified according to the number of real and repeated characteristic roots and the number of distinct compatibility relations.

If, along a curve C, in the x - t plane we write

$$\begin{aligned} du_1' &= u_1'' dx + \dot{u}_1' dt \\ d\dot{u}_1 &= \dot{u}_1' dx + \ddot{u}_1 dt \\ du_2' &= u_2'' dx + \dot{u}_2' dt \\ d\dot{u}_2 &= \dot{u}_2' dx + \ddot{u}_2 dt \ , \end{aligned} \tag{15}$$

then equations (14) and (15) form a system of six equations in the six unknowns u_1'', u_2'', $\ddot{u}_1$, $\ddot{u}_2$, $\dot{u}_1'$, $\dot{u}_2'$. In matrix form:

$$\begin{bmatrix} A_1 & B_1 & C_1 & D_1 & E_1 & F_1 \\ A_2 & B_2 & C_2 & D_2 & E_2 & F_2 \\ 0 & 0 & dt & 0 & dx & 0 \\ 0 & 0 & 0 & dt & 0 & dx \\ dx & 0 & 0 & 0 & dt & 0 \\ 0 & dx & 0 & 0 & 0 & dt \end{bmatrix} \begin{bmatrix} u_1'' \\ u_2'' \\ \ddot{u}_1 \\ \ddot{u}_2 \\ \dot{u}_1' \\ \dot{u}_2' \end{bmatrix} = \begin{bmatrix} R_1 \\ R_2 \\ d\dot{u}_1 \\ d\dot{u}_2 \\ du_1' \\ du_2' \end{bmatrix} \tag{16}$$

Letting N denote the determinant of the coefficient matrix and M_i denote the determinant of the matrix obtained by replacing the i^{th} column of the coefficient matrix by the column vector on the right side of equation (16), the characteristic roots are the values $\frac{dt}{dx}$ which satisfy $N = 0$, and the compatibility relations are given by $M_i = 0$ ($i = 1, 2, \ldots, 6$) for each characteristic root.

Returning to the membrane and introducing

$$F = \frac{\xi\sigma_1}{p_o}\,\frac{1+\varepsilon_2}{1+\varepsilon_1}, \quad F_1 = \frac{\partial F}{\partial \varepsilon_1}, \quad F_2 = \frac{\partial F}{\partial \varepsilon_2} \tag{17}$$

$$u = \frac{\partial \eta}{\partial \eta_o}, \quad v = \frac{\partial \omega}{\partial \eta_o}, \quad x = \frac{\partial \eta}{\partial \tau}, \quad y = \frac{\partial \omega}{\partial \tau},$$

the equations of motion can be written

$$\begin{aligned} &\eta_o \frac{\partial x}{\partial \tau} - \eta_o \left(F + \frac{u^2}{1+\varepsilon_1} F_1\right) \frac{\partial u}{\partial \eta_o} - \eta_o \frac{uv}{1+\varepsilon_1} F_1 \frac{\partial v}{\partial \eta_o} \\ &\qquad + (1+\varepsilon_1)\frac{\sigma_2}{p_o}\xi - \eta\frac{p}{p_o} v - uF + u(1+\varepsilon_2-u) F_2 = 0 \\ &-\eta_o \frac{\partial y}{\partial \tau} + \eta_o \frac{uv}{1+\varepsilon_1} F_1 \frac{\partial u}{\partial \eta_o} + \eta_o \left(F + \frac{v^2}{1+\varepsilon_1} F_1\right) \frac{\partial v}{\partial \eta_o} \\ &\qquad - \eta\frac{p}{p_o} u + vF - v(1+\varepsilon_2-u) F_2 = 0. \end{aligned} \tag{18}$$

Now letting $u_1 = \eta$, $u_2 = \omega$ and solving $N = 0$ yields the four characteristics roots

$$\frac{d\eta_o}{d\tau} = \pm \sqrt{F} \tag{19}$$

$$\frac{d\eta_o}{d\tau} = \pm \sqrt{F + (1+\varepsilon_1)F_1} \tag{20}$$

which are identical to those obtained by Cristescu [4]. Denoting the wave speeds by C_I and C_{II}, we have

$$C_I^2 = F = \frac{1+\varepsilon_2}{1+\varepsilon_1} \frac{\xi\sigma_1}{p_o} \tag{21}$$

$$C_{II}^2 = F + (1+\varepsilon_1)F_1 = \frac{1+\varepsilon_2}{p_o} \frac{\partial(\xi\sigma_1)}{\partial\varepsilon_1} \tag{22}$$

For the problem being considered, the pressure is constantly applied and hence there is no unloading. Thus, the characteristic roots given by equations (19) and (20) are real since ε_1, ε_2 and σ_1 are always positive.

Substituting each of the characteristic roots into $M_i = 0$ $(i = 1,2,....,6)$ yields four distinct compatibility relations:

$$\pm C_I(\omega_{\eta_o} d\eta_{\eta_o} - \eta_{\eta o}) - (\omega_{\eta_o} d\eta_\tau - \eta_{\eta_o} d\omega_\tau) - \frac{1+\varepsilon_1}{\eta_o p_o} \{\sigma_2 \omega_{\eta_o} - (1+\varepsilon_1) p\eta\} d\tau = 0 \tag{23}$$

$$\pm C_{II}(\eta_{\eta_o} d\eta_{\eta_o} + \omega_{\eta_o} d\omega_{\eta_o}) - (\eta_{\eta_o} d\eta_\tau + \omega_{\eta_o} d\omega_\tau) - \frac{1+\varepsilon_1}{\eta_o} \{\xi \frac{\sigma_2}{o} \eta_{\eta_o} + (1+\varepsilon_1)(1+\varepsilon_2 - \eta_{\eta_o}) F_2 - (1+\varepsilon_1) F\} d\tau = 0, \tag{24}$$

where the subscripts denote differentiation. The relations (23) and (24) are satisfied along the characteristics (19) and (20), respectively. Equations (23) differ from equations (5.19), (5.31) and (5.32) given by Cristescu [4], page 321-2, in that he obtained η_o rather than η in the last term on the left hand side. However, Cristescu's equation (5.29)

contains the correct term, η. Identical errors are found in the paper by Cristescu and Suliciu [11]. For large radial motion, this discrepancy could cause appreciable error in the numerical results.

From the above analysis, it is seen that the membrane equations have four real characteristic roots and four distinct compatibility relations. The system is said to be completely hyperbolic and may be solved by the method of characteristics (Chou and Perry [7]).

By considering the jump relations, Cristescu [4] has shown that the characteristics defined by equations (19) are transverse wave fronts that affect the shape of the membrane, and those given by equations (20) represent longitudinal wave fronts which produce an extension of the membrane.

Numerical Procedure

For numerical calculation, the $\eta_o - \tau$ plane is divided into a network by the characteristic lines, and the characteristic and compatibility equations are written in finite difference form in terms of the dependent variables at the mesh points of the network. There are four families of characteristic lines, with each characteristic intersecting every one of the other three characteristic families. The resulting network is too complex for practical calculation, and, for simplicity, only C^+_{II} and C^-_{II} characteristics are used as the main network. At the mesh points of the main network, the C^+_I and C^-_I characteristics are also drawn, and both sets of characteristic relations are then used to calculate the dependent variables at the mesh points

(Chou and Mortimer [8]). A conceptual model of the network is shown in Figure 5; the characteristics are represented as straight lines for illustrative purposes only, since in reality they are functions of strain.

The numerical procedure will be outlined in reference to Figure 6, which represents an interior loop of the network. The values of all required functions at points 1, 2 and 3 are known from previous calculations, and we seek the values of all variables at point 4. The characteristic lines 1-4 and 3-4 are approximated as straight lines, calculating the slopes using the values of ε_1 and ε_2 at points 1 and 3, respectively. Once the slopes are known, equations (20) are solved simultaneously to give $\eta_o(4)$ and $\tau(4)$.

In order to locate points 5 and 6 in the $\eta_o - \tau$ plane, the lines 5-4 and 6-4 are also approximated as straight lines using the values $\varepsilon_1 = \frac{1}{2}[\varepsilon_1(1) + \varepsilon_1(3)]$ and $\varepsilon_2 = \frac{1}{2}[\varepsilon_2(1) + \varepsilon_2(3)]$ to calculate the slopes. Equations (19) and (20) are then written as

$$\begin{aligned} [\eta_o(4) - \eta_o(5)] &= C_I[\tau(t) - \tau(5)] \\ [\eta_o(1) - \eta_o(5)] &= - C_{II}[\tau(1) - \tau(5)], \end{aligned} \tag{25}$$

and are solved simultaneously for $\eta_o(5)$ and $\tau(5)$. Similar relations written along 6-4 and 6-3 are solved simultaneously for $\eta_o(6)$ and $\tau(6)$.

Using the now known locations of 5 and 6, linear interpolation along 2-1 and 2-3 is used to obtain all required functional values at points 5 and 6, respectively. Specifically, the values obtained are the two spatial derivatives, two time derivatives and the strain com-

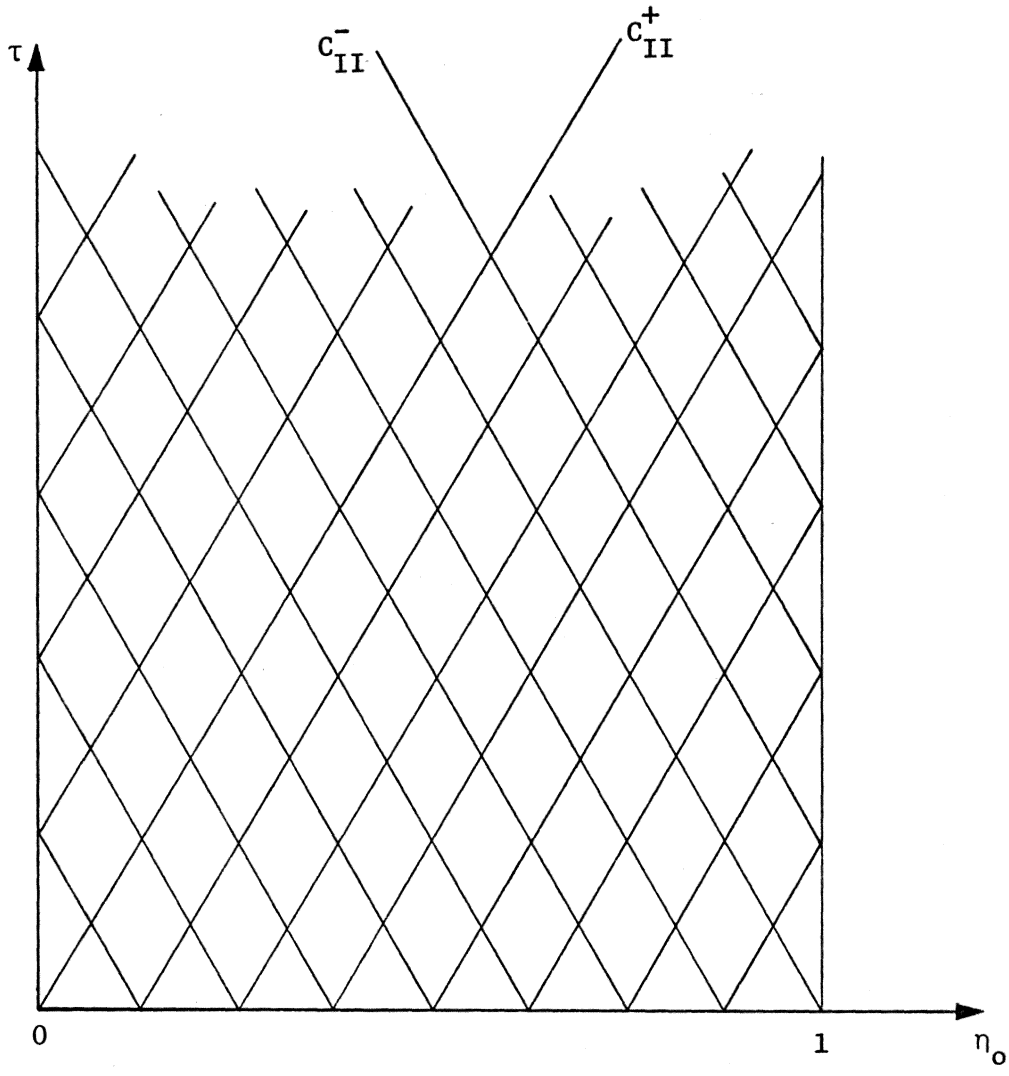

Figure 5. Main characteristic mesh.

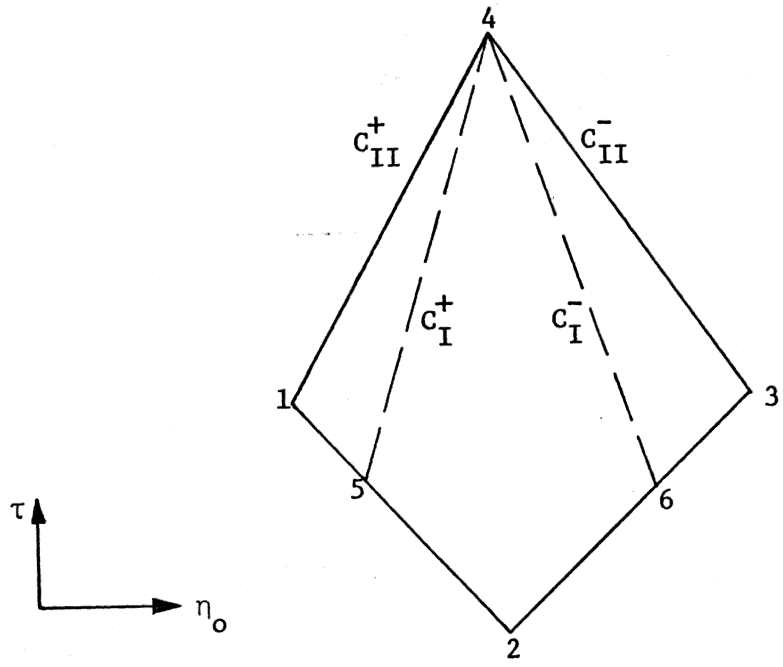

Figure 6. Interior loop of the characteristic network.

ponents. We now have sufficient information to complete the solution at point 4.

The four basic unknowns at point 4 are the derivatives $\eta_{\eta o}$, $\omega_{\eta o}$, η_τ and ω_τ. With equations (23) and (24) written in finite difference form along the proper characteristic lines, we have a system of four equations involving the four derivatives at point 4 and the known quantities at 1, 3, 5 and 6. Simultaneous solution of this system yields $\eta_{\eta o}(4)$, $\omega_{\eta o}(4)$, $\eta_\tau(4)$ and $\omega_\tau(4)$. The actual coordinates of point 4 are now calculated from the relations

$$\begin{aligned} d\eta &= \frac{\partial \eta}{\partial \eta_o} d\eta_o + \frac{\partial \eta}{\partial \tau} d\tau \\ d\omega &= \frac{\partial \omega}{\partial \eta_o} d\eta_o + \frac{\partial \omega}{\partial \tau} d\tau \end{aligned} \tag{26}$$

integrated as finite differences along C_{II} and C_I characteristics, respectively.

The strain components $\varepsilon_1(4)$ and $\varepsilon_2(4)$ are computed from the defining equations (9), and $\varepsilon_3(4)$, $\sigma_1(4)$ and $\sigma_2(4)$ are found from the constitutive relation written in the form of equations (12).

A second iteration is now made to find the solution to a closer approximation. The procedure is the same as before except the slopes 1-4 and 3-4 are calculated using

$$\begin{aligned} \varepsilon_1 &= \frac{1}{2} [\varepsilon_1(1) + \varepsilon_1(4)] \\ \varepsilon_1 &= \frac{1}{2} [\varepsilon_1(3) + \varepsilon_1(4)] \end{aligned} \tag{27}$$

and similarly for ε_2. The value of C_I is calculated using the values $\varepsilon_1(4)$ and $\varepsilon_2(4)$ from the first approximation.

At the right hand boundary, Figure 7, two of the characteristics are missing. However, since $\eta_\tau = \omega_\tau = 0$ and $\eta = \eta_o = 1$ are known from the boundary conditions, the two characteristics that are available are sufficient to solve for all unknown quantities. The value of τ is found by integrating (20) along the C^+_{II} characteristic. By solving simultaneously equations (23) and (24) along C^+_I and C^+_{II}, the values of $\eta_{\eta o}$ and $\omega_{\eta o}$ are found.

The conditions of symmetry along the line $\eta_o = 0$ are such that this line may be treated as a boundary also. The boundary conditions used along this line are: $\eta = \eta_o = 0$ and $\eta_\tau = \omega_{\eta o} = 0$. Thus, the two characteristics available at $\eta_o = 0$ are also sufficient for calculating all unknowns.

Alternate Numerical Procedure

An alternate numerical procedure as outlined by Cristescu [4] may be realized if the compatibility equations (23) and (24) are rewritten in a different form. Introducing the relation

$$\omega_{\eta_o}\, d\eta_{\eta_o} - \eta_{\eta_o}\, d\omega_{\eta_o} = \omega_{\eta_o}^2\, d\left(\frac{\eta_{\eta_o}}{\omega_{\eta_o}}\right) \tag{28}$$

and, from Figure 4,

$$\frac{\eta_s}{\omega_s} = \frac{\eta_{\eta_o}}{\omega_{\eta_o}} = \cot \Phi_1 \,, \tag{29}$$

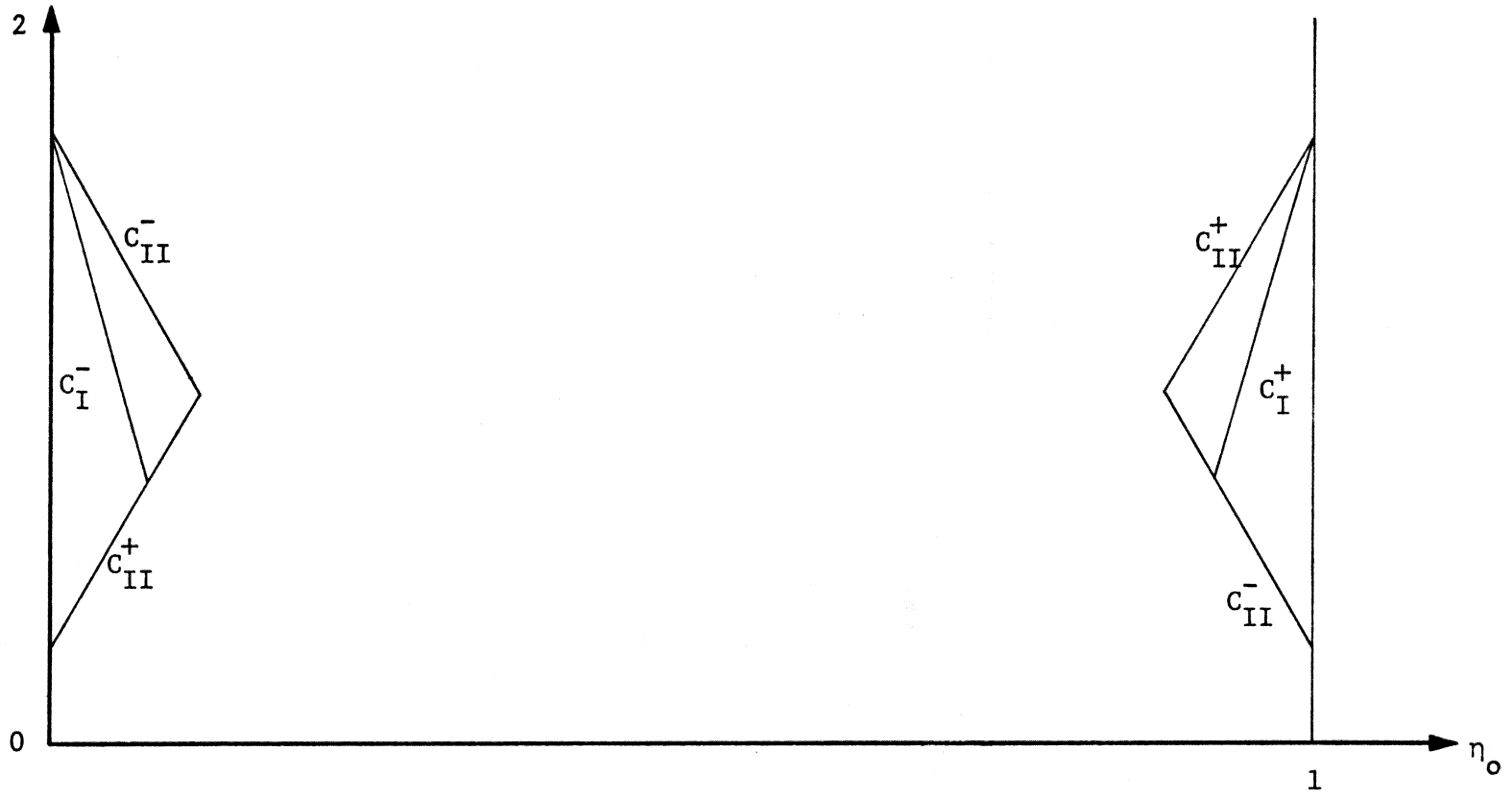

Figure 7. Characteristic mesh at the boundaries.

we can write

$$\omega_{\eta_o} \, d\eta_{\eta_o} - \eta_{\eta_o} \, d\omega_{\eta_o} = \omega_{\eta_o}^2 \, d \, (\cot \Phi_1). \tag{30}$$

Recalling the definition of the meridional strain

$$\varepsilon_1 = \sqrt{\eta_{\eta_o}^2 + \omega_{\eta_o}^2} \; - 1 \; , \tag{31}$$

and introducing ε_1 into equation (30) yields

$$\begin{aligned} \omega_{\eta_o} \, d\eta_{\eta_o} - \eta_{\eta_o} \, d\omega_{\eta_o} &= (1+\varepsilon_1)^2 \, \frac{d(\cot \Phi_1)}{1 + (\cot \Phi_1)^2} \\ &= - (1+\varepsilon_1) \, d \, \Phi_1. \end{aligned} \tag{32}$$

If $\vec{R}$ denotes the position vector of a point on the membrane of Figure 4, we may write

$$\vec{R} = \eta \vec{e}_1 + \omega \vec{e}_2 \tag{33}$$

where $\vec{e}_1$ and $\vec{e}_2$ are unit vectors in the r and z directions, respectively. Differentiating (33) with respect to the non-dimensionalized arc length ψ we obtain

$$\frac{d\vec{R}}{d\psi} = \eta_\psi \vec{e}_1 + \omega_\psi \vec{e}_2 = \frac{1}{1+\varepsilon_1} \, (\eta_{\eta_o} \vec{e}_1 + \omega_{\eta_o} \vec{e}_2) \; . \tag{34}$$

The velocity of the point considered is

$$\vec{v} = \frac{d\vec{R}}{d\tau} = \eta_\tau \vec{e}_1 + \omega_\tau \vec{e}_2, \tag{35}$$

and the unit vectors normal and tangential to the membrane are given by

$$\vec{e}_n = - \omega_\psi \vec{e}_1 + \eta_\psi \vec{e}_2 = \frac{1}{1+\varepsilon_1} \, (-\omega_{\eta_o} \vec{e}_1 + \eta_{\eta_o} \vec{e}_2) \tag{36}$$

$$\vec{e}_T = \eta_\psi \vec{e}_1 + \omega_\psi \vec{e}_2 = \frac{1}{1+\varepsilon_1} (\eta_{\eta_o} \vec{e}_1 + \omega_{\eta_o} \vec{e}_2) . \tag{37}$$

Writing equation (35) in differential form

$$d\vec{v} = d\eta_\tau \vec{e}_1 + d\omega_\tau \vec{e}_2 \tag{38}$$

The normal and tangential velocity components are then given by

$$(d\vec{v})_n = (d\vec{v}) \cdot \vec{e}_n = - \frac{1}{1+\varepsilon_1} (\omega_{\eta_o} d\eta_\tau - \eta_{\eta_o} d\omega_\tau) \tag{39}$$

$$(d\vec{v})_T = (d\vec{v} \cdot \vec{e}_T) = \frac{1}{1+\varepsilon_1} (\eta_{\eta_o} d\eta_\tau + \omega_{\nu_o} d\omega_\tau) \tag{40}$$

respectively. For use in the compatibility relations, equations (39) and (40) are written as

$$\omega_{\eta_o} d\eta_\tau - \eta_{\eta_o} d\omega_\tau = - (1+\varepsilon_1) (d\vec{v})_n \tag{41}$$

$$\eta_{\eta_o} d\eta_\tau + \omega_{\eta_o} d\omega_\tau = (1+\varepsilon_1) (d\vec{v})_T . \tag{42}$$

Finally, using equation (31), we have

$$\eta_{\eta_o} d\eta_{\eta_o} + \omega_{\eta_o} d\omega_{\eta_o} = (1+\varepsilon_1) d\varepsilon_1 . \tag{43}$$

Substituting equations (32), (41), (42) and (43) into equations (23) and (24), the compatibility relations become

$$\pm C_I d\Phi_1 + (d\vec{v})_n - \frac{1}{\eta_o p_o} \{\xi\sigma_2 \omega_{\eta_o} - (1+\varepsilon_1) p\eta\} d\tau = 0 \tag{44}$$

$$\pm C_{II} d\varepsilon_1 - (d\vec{v})_T - \frac{1}{\eta_o} \{\xi \frac{\sigma_2}{p_o} \eta_{\eta_o} + (1+\varepsilon_1) (1+\varepsilon_2 - \eta_{\eta_o}) F_2 - (1+\varepsilon_1) F\} d\tau = 0. \tag{45}$$

In this form, the compatibility relations show that on the transverse wave fronts the variations in the angle Φ_1 and the normal velocity component are related, while on the longitudinal wave fronts the variations in radial strain and tangential velocity are related.

In order to solve numerically for the desired variable values, equation (44) will be written in a different form. Solving equations (42) and (43) for $d\omega_{\eta_o}$ and $d\omega_\tau$ and substituting in (44) yields

$$\pm C_I \, d\eta_{\eta_o} - d\eta_\tau - \frac{\eta_{\eta_o}}{1+\varepsilon_1} \left[\pm C_I \, d\varepsilon_1 - (d\vec{v})_T\right] - \frac{\omega_{\eta_o}}{(1+\varepsilon_1)\,\eta_o\,p_o} \left\{\xi\sigma_2\,\omega_{\eta_o} - (1+\varepsilon_1)\,p\eta\right\} \, d\tau = 0. \tag{46}$$

Similarly, solving for $d\eta_{\eta_o}$ and $d\eta_\tau$ and substituting gives

$$\pm C_I \, d\omega_{\eta_o} - d\omega_\tau - \frac{\omega_{\eta o}}{1+\varepsilon_1} \left[\pm C_I \, d\varepsilon_1 - (d\vec{v})_T\right] + \frac{\eta_{\eta_o}}{(1+\varepsilon_1)\eta_o p_o} \left\{\xi\sigma_2 \, \omega_{\eta_o} - (1+\varepsilon_1)\,p\eta\right\} \, d\tau = 0. \tag{47}$$

When written in finite difference form along the proper characteristic lines, equations (45), (46) and (47) form a system of six equations in the six unknowns ε_1, v_T, η_{η_o}, η_τ, ω_{η_o} and ω_τ. Following a procedure similar to that previously outlined, the six equations are solved to give the values of the six variables at each mesh point of the main characteristic network. The alternate numerical procedure was not used in this work as it involves more programming effort and since the first procedure gave satisfactory results. The alternate approach is detailed here, however, since it may be more appropriate for different loadings or initial conditions.

Linearly Elastic Action

The analysis will now be restricted to an isotropic, linearly elastic membrane. For such a material, the stress-strain relation as given by Frederick and Chang [9] is

$$\sigma_{ij} = \frac{E}{1+\nu} \left[\varepsilon_{ij} + \frac{\nu}{1-2\nu} \varepsilon_{kk} \delta_{ij}\right] \qquad (i,j = 1,2,3) \tag{48}$$

where E is the modulus of elasticity, ν is Poisson's ratio, ε_{kk} is the first strain invariant and δ_{ij} is the Kronecker delta.

The principal stresses in the membrane may now be written in definite form, and equations (11) become

$$\begin{aligned} \sigma_1 &= \frac{E}{1-\nu^2} (\varepsilon_1 + \nu\, \varepsilon_2) \\ \sigma_2 &= \frac{E}{1-\nu^2} (\varepsilon_2 + \nu \varepsilon_1) \\ \sigma_3 &= 0 \ , \end{aligned} \tag{49}$$

and equation (13) is

$$\varepsilon_3 = \frac{\nu}{\nu-1} (\varepsilon_1 + \varepsilon_2) \ . \tag{50}$$

Substituting in equations (21) and (22) yields for the wave speeds

$$\begin{aligned} C_I^2 &= \frac{E}{1-\nu^2} \frac{1}{p_o} \frac{1+\varepsilon_2}{1+\varepsilon_1} (1+\varepsilon_3) (\varepsilon_1 + \nu\varepsilon_2) \\ C_{II}^2 &= \frac{E}{1-\nu^2} \frac{1+\varepsilon_2}{p_o} \left\{\frac{\nu}{\nu-1} [2\varepsilon_1 + (1+\nu)\, \varepsilon_2] + 1\right\} \ . \end{aligned} \tag{51}$$

For values of ν in the physically meaningful range, $(-1<\nu<\frac{1}{2})$, it can be shown that $C_{II} > C_I$, provided the values of strain do not exceed

50%. Thus, it is certainly reasonable to assume that C_{II} is always greater than C_I for the elastic case. This is significant since the numerical procedure previously outlined is valid only for $C_{II} > C_I$. If, at some instant, $C_I > C_{II}$, the C_I characteristic mesh would become the main network, and the numerical procedure would change. Two programs would be required, and automatic switching would be necessary.

Initial Conditions

A small radial extension is performed, and the membrane is then clamped along a boundary of radius R. Thus, there is an initial radial stress, σ_1, which will be denoted by T_o. The initial conditions are then

$$\sigma_1 = \sigma_2 = T_o \qquad \eta = \eta_o$$

$$\varepsilon_1 = \varepsilon_2 = \frac{1-\nu}{E} T_o \qquad \omega = 0 \tag{52}$$

$$\varepsilon_3 = -\frac{2\nu}{E} T_o$$

and

$$C_I^2 = (1 - \frac{2\nu}{E} T_o) \frac{T_o}{p_o} \tag{53}$$

$$C_{II}^2 = \frac{E+(1-\nu)T_o}{E} \frac{E - 4\nu\, T_o}{(1-\nu)\, p_o} \quad .$$

The second of equations (53) differs from that given by Cristescu [4] since the term $(1-\nu)$ in the denominator replaces the term $(1-\nu^2)$.

IV. RESULTS

Physical Parameters

The numerical solution obtained is for a membrane material having physical properties:

Elastic modulus, $E = 10 \times 10^6$ psi

Poisson's ratio, $\nu = 0.3$

Mass density, $\rho_o = 0.003$ slugs/in^3

The properties selected correspond approximately to hard-drawn aluminum having a proportional limit in tension of 20,000 psi (Timoshenko and Young [10]).

The pressure input is $p_o = 20{,}000$ psi. Note that this is not actual pressure, but is related to actual pressure through the scaling equation

$$p_o = \frac{P_o R}{h_o} \quad , \tag{54}$$

where P_o is the actual pressure, R is the membrane radius and h_o is the initial membrane thickness. The scaling used makes possible the examination of a large number of pressure-radius-thickness combinations through the single parameter p_o. Some of the possible combinations are shown in Table I for $p_o = 20{,}000$ psi. The results are interpreted for a 6 inch diameter membrane, 0.005 inch thick, which is subjected to an impulsive pressure of 33.3 psi.

TABLE I. Some possible pressure-radius-thickness combinations corresponding to p_o = 20,000 psi.

P_o (psi)	R (in)	h_o (in)
10.0	3	0.0015
20.0	3	0.003
33.3	3	0.005
333.3	3	0.050
10.0	4	0.002
20.0	4	0.004
30.0	6	0.009

Numerical Convergence Data

The numerical calculations were performed on an IBM 360/65 digital computer using the Fortran IV programming language. Since the characteristics are functions of strain, it was not possible to draw them a priori, nor was it possible to perform the calculations using either a fixed time or space increment. Only the initial number of space intervals along the radius of the membrane may be specified; the location of subsequent points in both time and space being determined by the program itself.

The initial number of spatial intervals was increased with each computer run in order to make the characteristic mesh finer each time. Increasing the number of intervals decreases both time and space increments between each calculation and should improve accuracy each time. In order to determine convergence, the meridional stress, σ_1, was selected as the criterion variable. The stress component was selected because it reflects changes in both ε_1 and ε_2, and should be highly sensitive since it is determined using a large coefficient involving the modulus of elasticity. The vertical and radial displacements were considered as convergence variables but rejected as they are small when considering the elastic case and do not truly reflect convergence. The various derivatives were also rejected as convergence variables since all are directly involved in calculating ε_1 and ε_2 and hence are reflected in the value of the meridional stress.

The initial set of calculations was performed with the radius divided into 20 equal intervals; that is, $\Delta\eta_o = 0.05$. Subsequent

calculations used 40, 80, 120, 160 and 320 initial intervals. After each run, the spatial distribution of meridional stress was plotted for a fixed time after application of the load. By superposing the stress distribution for each run, it was determined that convergence was obtained for 160 initial space intervals. The meridional stress distribution for the various runs is shown in Figure 8. Another method of determining convergence is to plot the stress at a given spatial point versus initial interval size. This plot is shown in Figure 9.

Propagation of the Strain Wave

As stated in the analysis of the governing equations, the C_{II} characteristic families represent longitudinal waves which produce an extension, or straining, of the membrane. In Figure 10 is shown the leading C_{II}^{-} characteristic which emanates from the fixed boundary at $t = 0$. This characteristic represents the initial strain wave which propagates toward the center as the membrane deflects upward and hence must be extended since it is fixed around the periphery. At $t = 13$ microseconds, the leading wave front has reached the center of the membrane and appears to be reflected outward. In actuality, the "reflected" wave is the wave front which originated at a point diametrically opposite on the fixed boundary and has now passed through the center of the membrane. This wave front then propagates outward until, at $t = 26$ microseconds, it is reflected inward from the boundary. The reflected characteristic is not drawn beyond $t = 28$ microseconds since beyond this time it is found that the values of the stresses in the membrane exceed

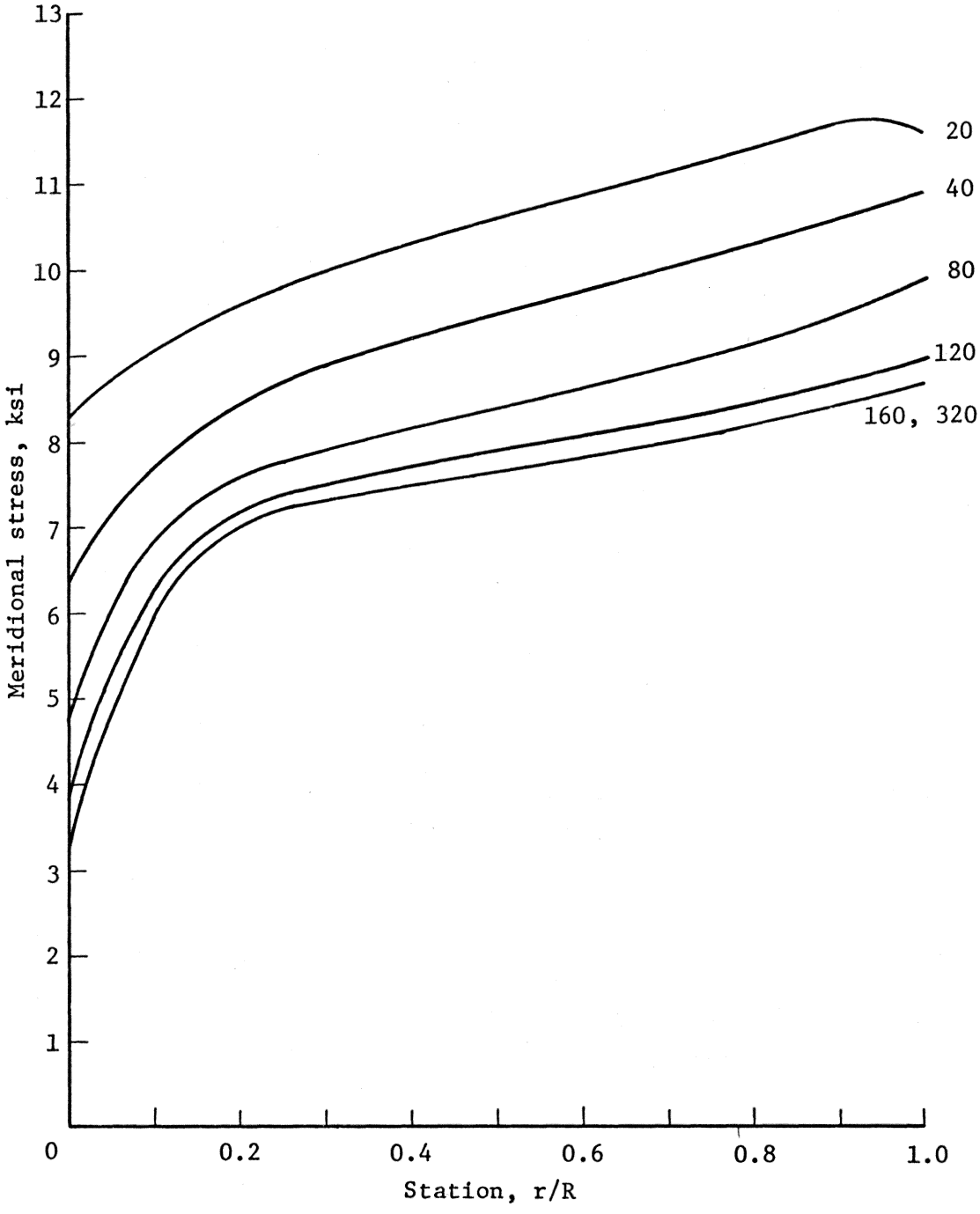

Figure 8. Meridional stress distribution illustrating convergence.

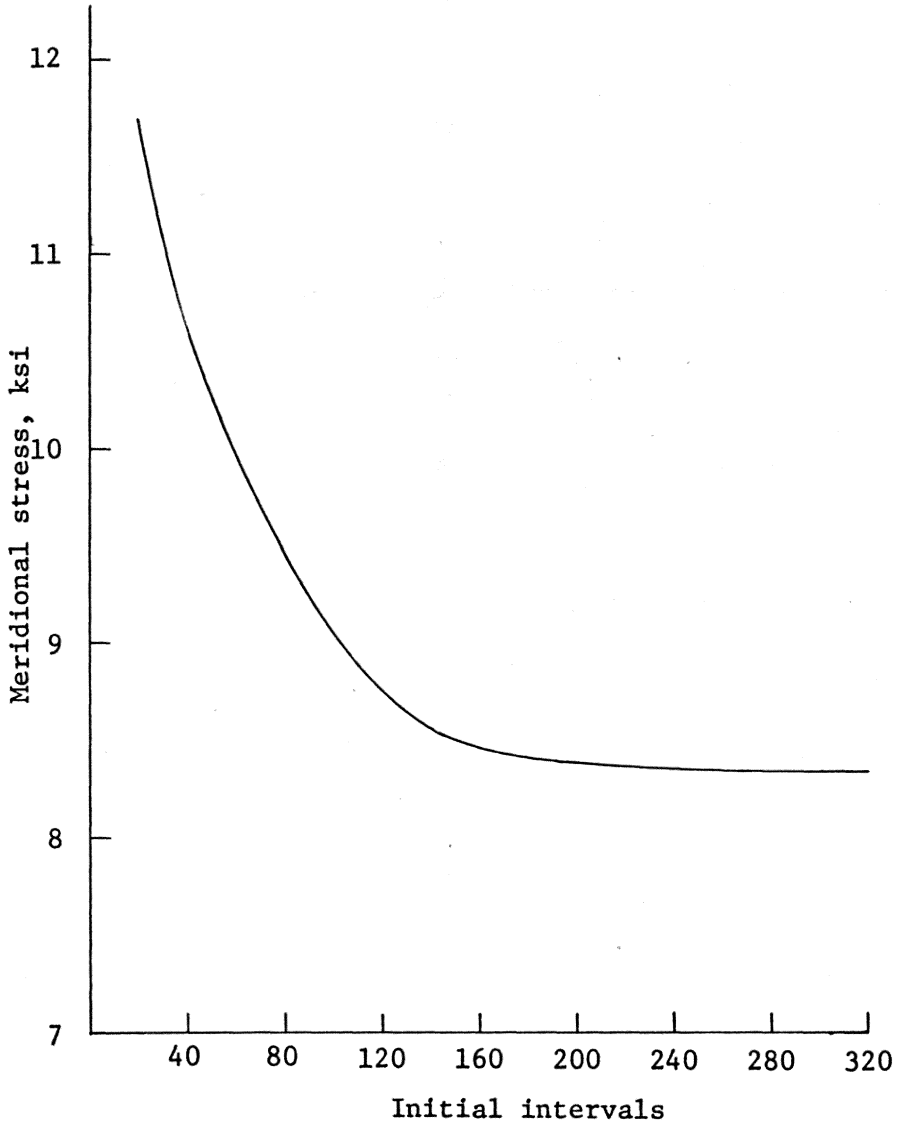

Figure 9. Alternate convergence data--meridional stress history at r/R = 0.9.

the elastic limit and the numerical procedure is no longer valid.

The numerical results show that the C_{II} characteristics are straight lines. Thus, the strain waves propagate with an essentially constant velocity during the elastic phase of the deformation. From the slope of the characteristics in Figure 10, the strain wave velocity is 2.3×10^5 inches per second. Recalling the last of equations (51)

$$C_{II}^2 = \frac{E}{1-\nu^2} \frac{1+\varepsilon_2}{p_o} \left\{\frac{\nu}{\nu-1} [2\varepsilon_1 + (1+\nu)\varepsilon_2] + 1\right\} , \tag{55}$$

if the values of the strain components are taken to be small in comparison to unity, substituting the values for E, ν and p_o results in $C_{II} = 2.3 \times 10^5$ inches per second which is in agreement with the value from the complete numerical solution.

The effect of the strain wave is seen by examining the state of stress in the membrane at various times. Figures 11 through 13 give the spatial distribution of meridional stress at successive time intervals during the deformation. As shown in Figure 11, at t = 5 microseconds the leading strain wave front has moved inward a distance of about 40% of the radius, and at this point the jump in the meridional stress component is 250 psi. To the left of the leading wave front, the stress state in the membrane remains unchanged from the initial conditions as in this portion the effect of the fixed boundary has not been felt. To the right of, or behind the wave front, a high gradient exists, with the stress increasing non-linearly toward the boundary. The increasing stress behind the leading wave front represents the action of successive wave fronts originating at the boundary and beginning to propagate

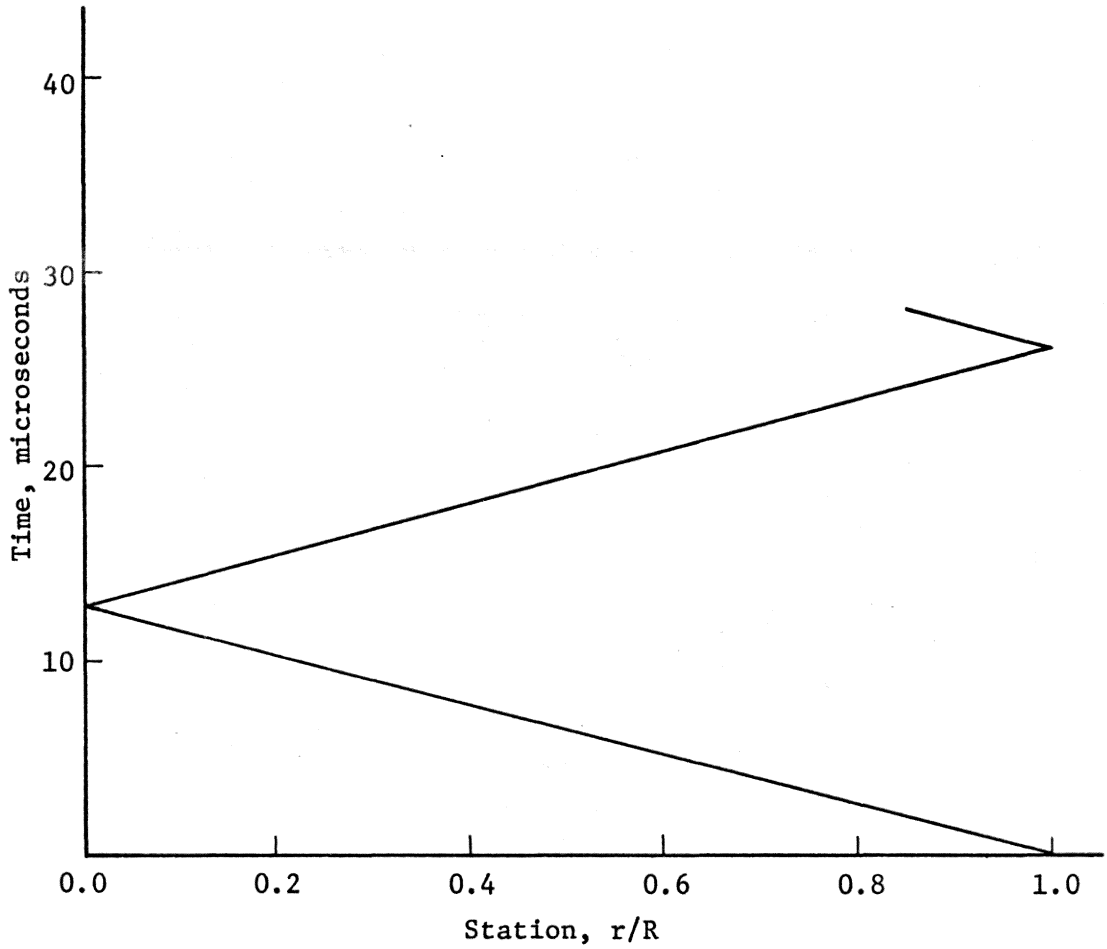

Figure 10. Leading C_{II}^{-} characteristic.

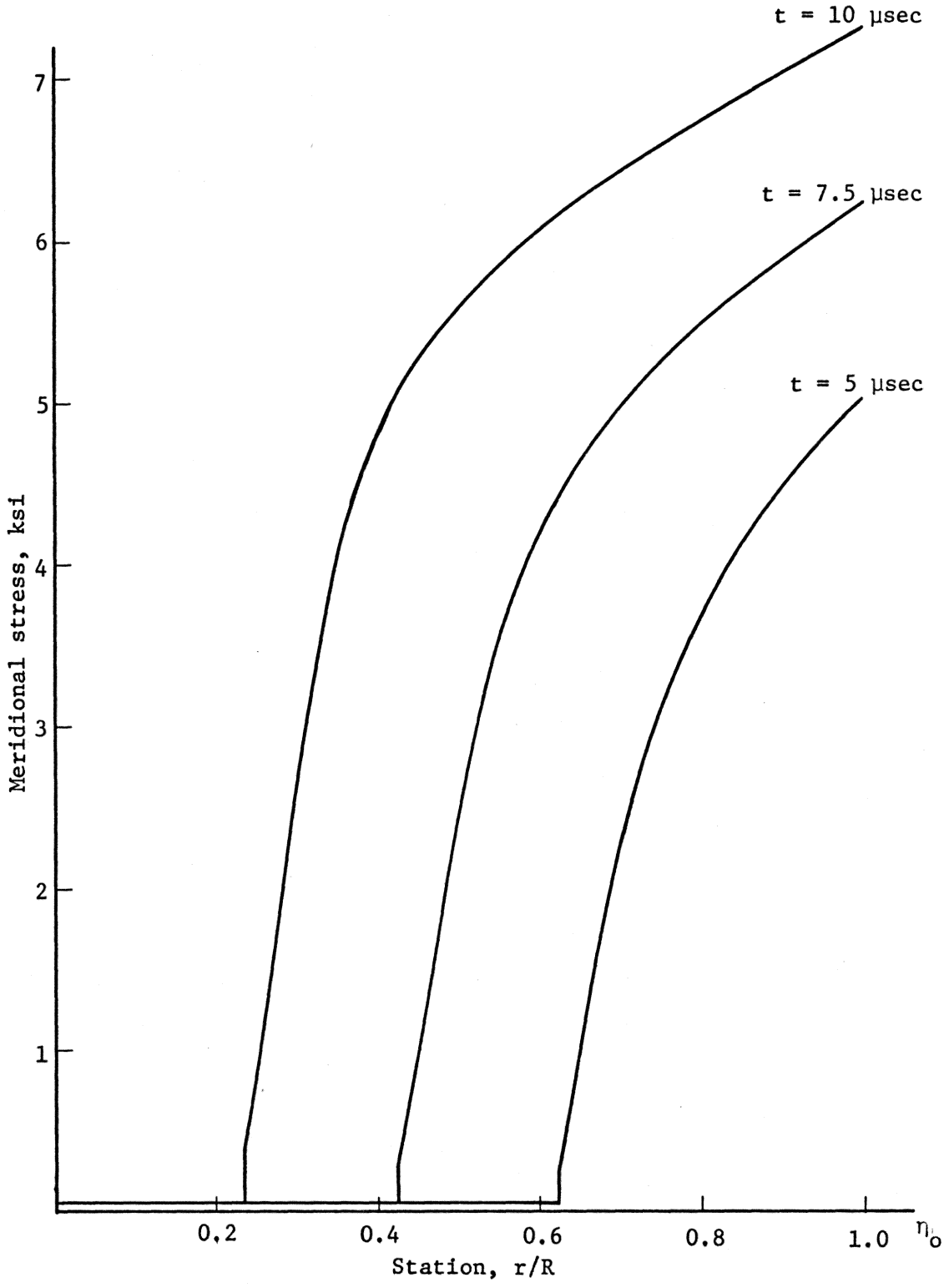

Figure 11. Meridional stress distribution at succeeding times.

across the membrane. As the leading wave front continues toward the center, the stress distribution behind it shifts upward and to the left while maintaining approximately the same shape. The jump in meridional stress increases inversely with the distance from the center of the membrane to the wave front and has increased to 750 psi when the wave front has moved across 95% of the radius.

Figure 12 shows that the leading wave front reaches the center of the membrane at t = 13 microseconds. At this time, two wave fronts moving diametrically toward each other interact to give a jump in stress of 3400 psi at the center. Following the interaction of the leading waves, the stress at the center increases very rapidly due to the arrival and interaction of succeeding wave fronts. At t = 15 microseconds the stress at the center has increased to a magnitude of 15,200 psi. The reflected wave front has started to move back toward the fixed boundary from the center. From Figure 12 at t = 16 microseconds and Figure 13 for 18, 20, 22, 24 and 26 microseconds, the outward movement of the reflected wave front is readily observed.

The stress distribution for t = 26 microseconds shows that the outer 25% of the membrane has been stressed beyond the elastic limit and yielding has occurred. A comparison with the last curve in Figure 13 shows that within 2 microseconds all points in the membrane have reached the yield state. Thus, the assumption made by Hudson, Frederick and others that the stress everywhere is equal to the yield stress appears to be justified from the numerical results for the elastic phase.

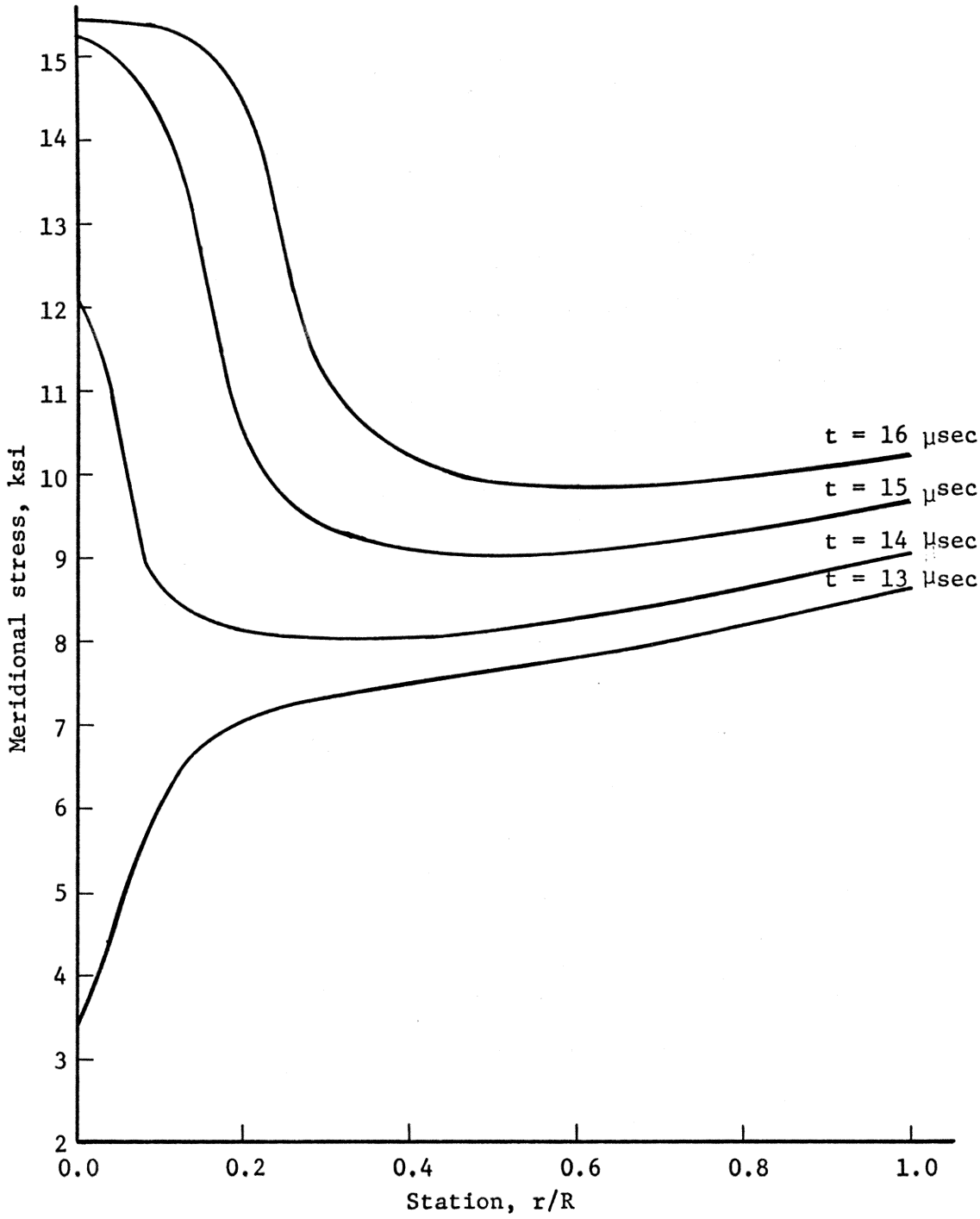

Figure 12. Meridional stress distribution at succeeding times.

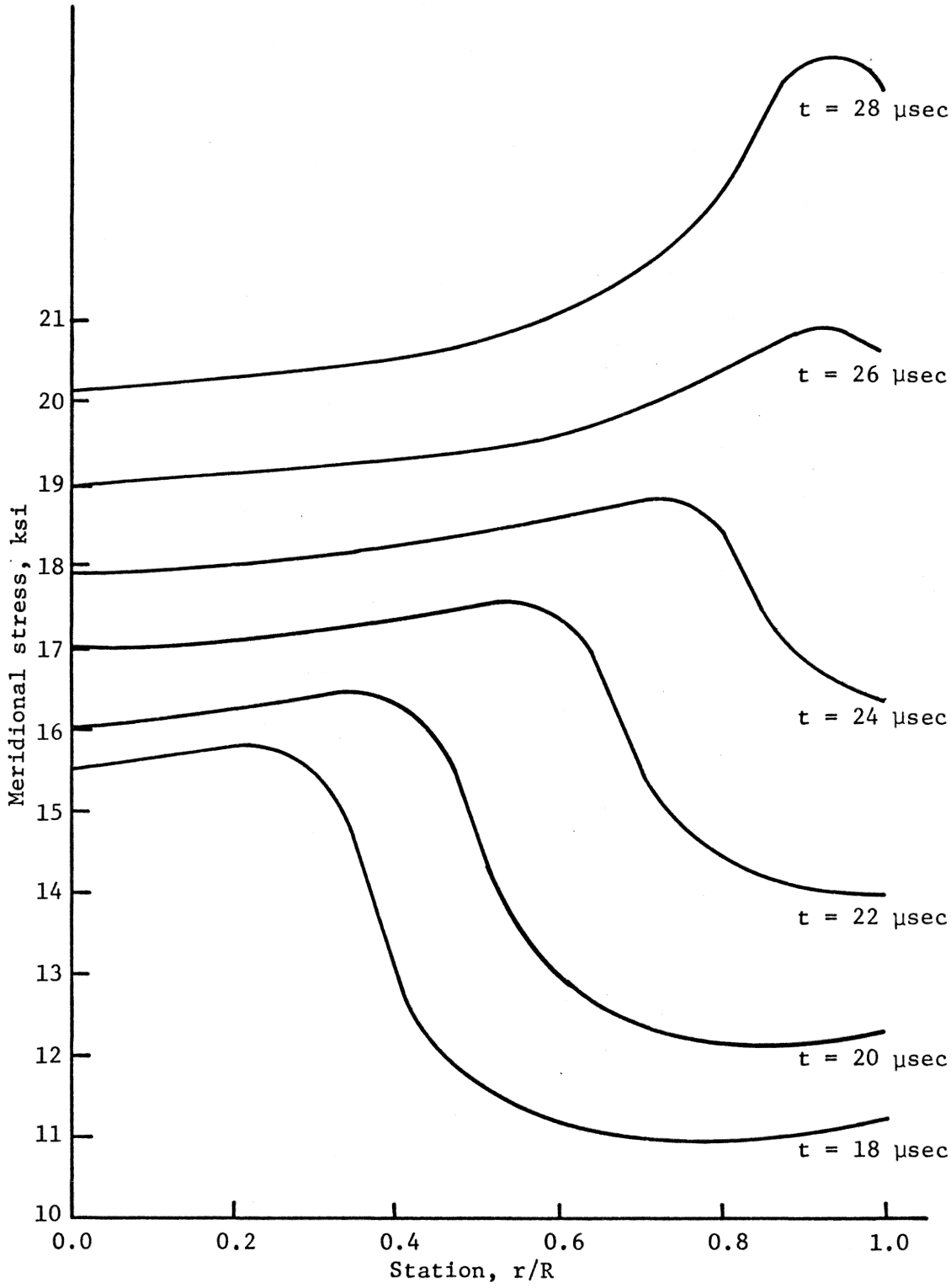

Figure 13. Meridional stress distribution at succeeding times.

In the latter stages of deformation, a negative gradient in meridional stress is noticeable near the boundary. This occurs, in fact, at all times although it is not shown on the figures due to the scale used. At the boundary, the circumference of the membrane is fixed; thus, the circumferential strain component is fixed at its initial value. In order to satisfy the boundary condition and maintain continuity, there exists a thin region at the outer edge of the membrane in which the circumferential strain increases rapidly. High gradients exist in both meridional and circumferential stress in this region as each is dependent on circumferential strain. As an example of this "boundary layer" effect, the meridional stress at t = 28 microseconds is 18,000 psi at the boundary while at $\frac{r}{R} = 0.98$ it is 24,000 psi.

Propagation of the Inertia Wave

The propagation of the inertia wave is evidenced by the changing shape of the membrane with time. Due to the fixed support along the periphery of the membrane, a discontinuity in slope develops and moves toward the center as the membrane deforms. This phenomenon corresponds to the hinge concept of Hudson and Frederick. The location of the discontinuity in slope at various times is shown in Figure 14. After an initial accelerating period of 4 microseconds, the discontinuity moves inward with a constant velocity of 12.2 in/msec as determined from the slope of the straight portion of the curve. At t = 28 microseconds, the slope discontinuity has propagated inward by a distance equal to 15% of the radius. As an example, this represents less than $\frac{1}{2}$ inch

for a six inch diameter membrane. The curve is not extended beyond t = 28 microseconds since the stresses exceed the elastic limit and the analysis is no longer valid.

That the location of the slope discontinuity is the point at which the effect of the fixed boundary is felt is verified by observing the axial velocity distribution across the membrane at various times. Velocity distributions at three different times are shown in Figures 15, 16 and 17. In each case, there is a central section of the membrane in which each point is moving upward with the same velocity, and an outer section in which the velocities decrease to zero at the fixed boundary. By direct comparison of Figure 14 with Figures 15, 16 and 17, the point at which the slope discontinuity occurs corresponds identically to the location at which the velocity changes from uniform to decreasing. It is interesting to note that the axial velocity curves are composed of two linear portions connected by a non-linear segment. This result is as expected since for the elastic case and the corresponding small deflections the non-linear behavior should be limited to the immediate vicinity of the wave front.

Since the inertia wave does not reach the center of the membrane during the elastic phase of deformation, the central portion remains flat, and the only force acting on it in the axial direction is the resultant of the applied pressure. Figure 18 shows the axial velocity of the center of the membrane which is seen to be a linearly increasing function of time. As measured by the slope of the velocity curve, the center of the membrane moves upward with a constant axial acceleration of 27 $in/msec^2$. A similar analysis shows that any point between the

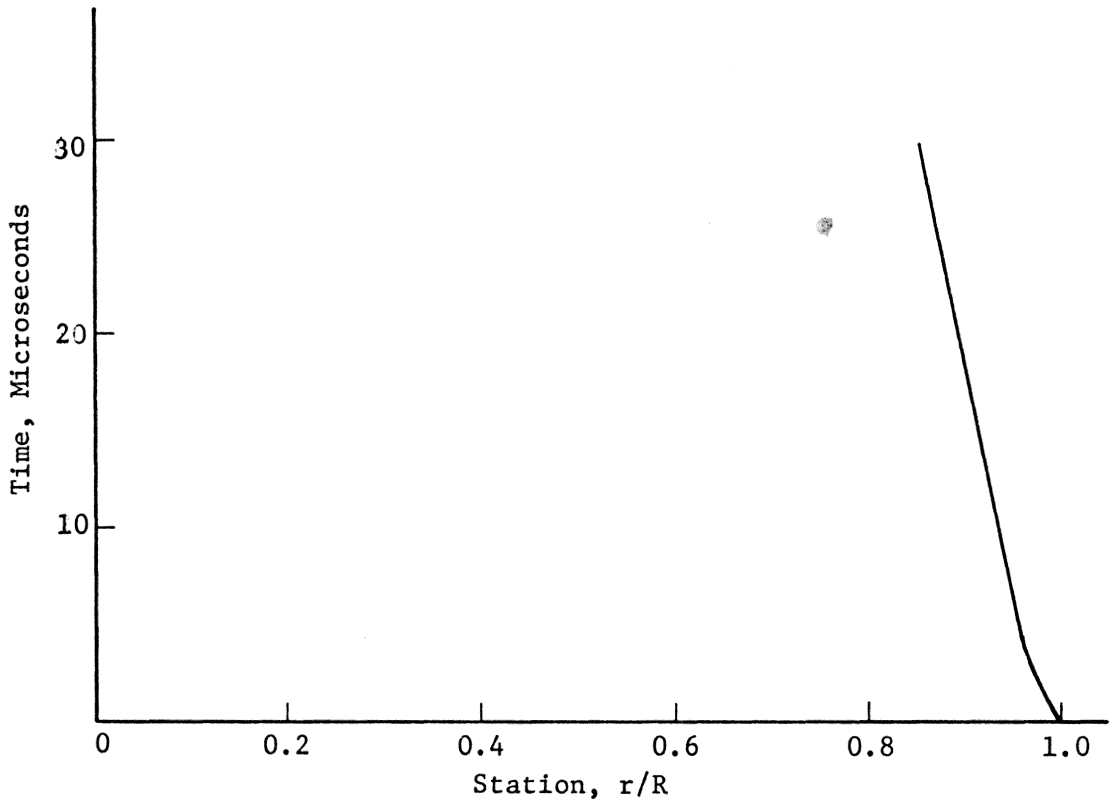

Figure 14. Position of slope discontinuity as a function of time.

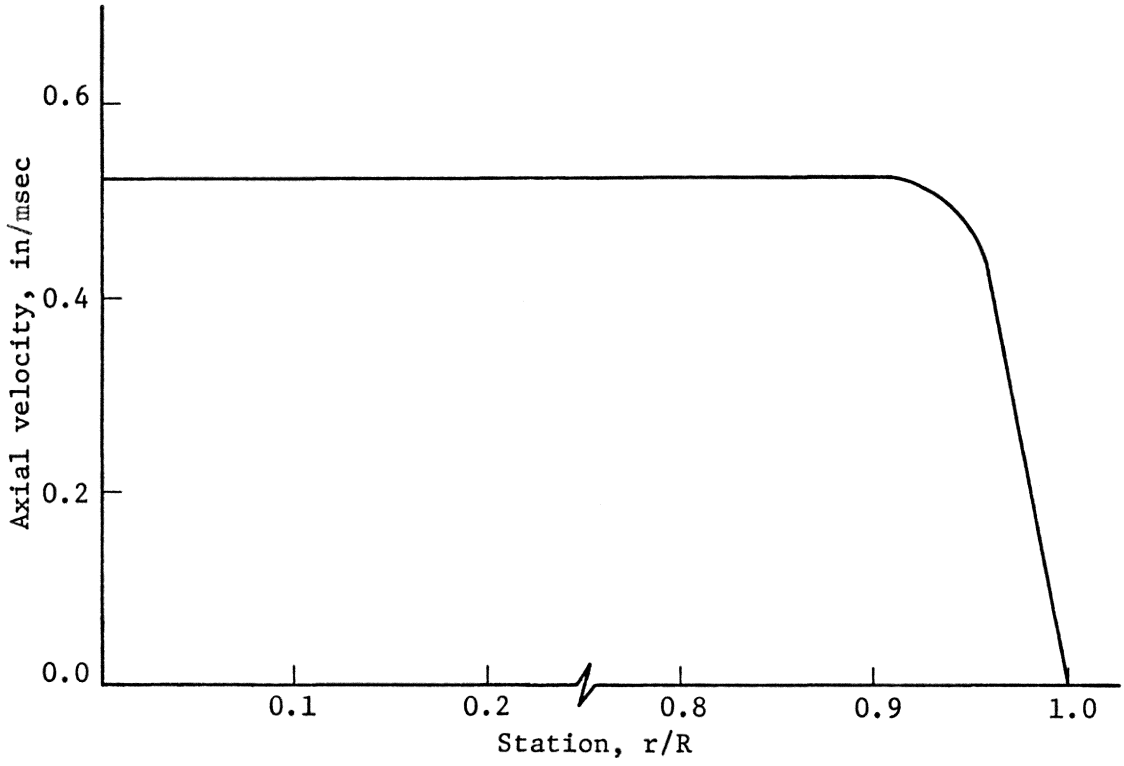

Figure 15. Axial velocity distribution at t = 20 microseconds.

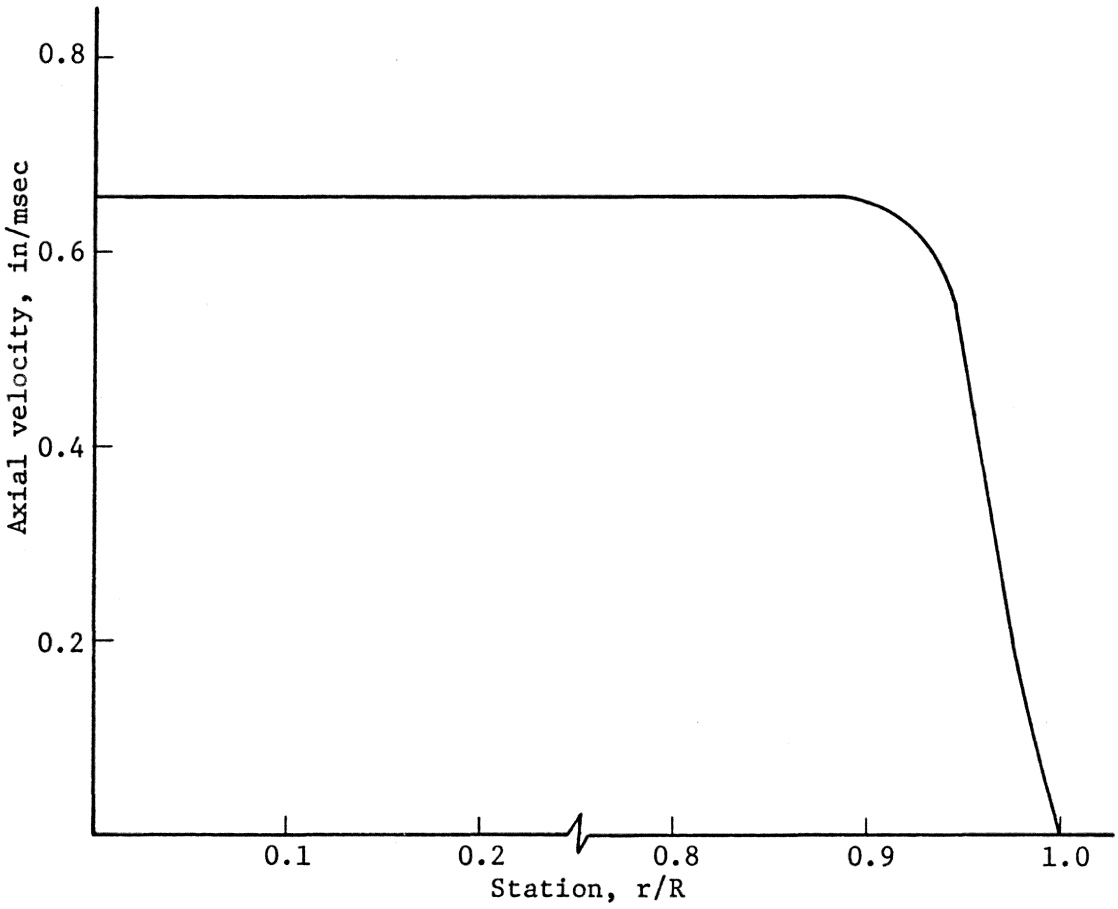

Figure 16. Axial velocity distribution at t = 25 microseconds.

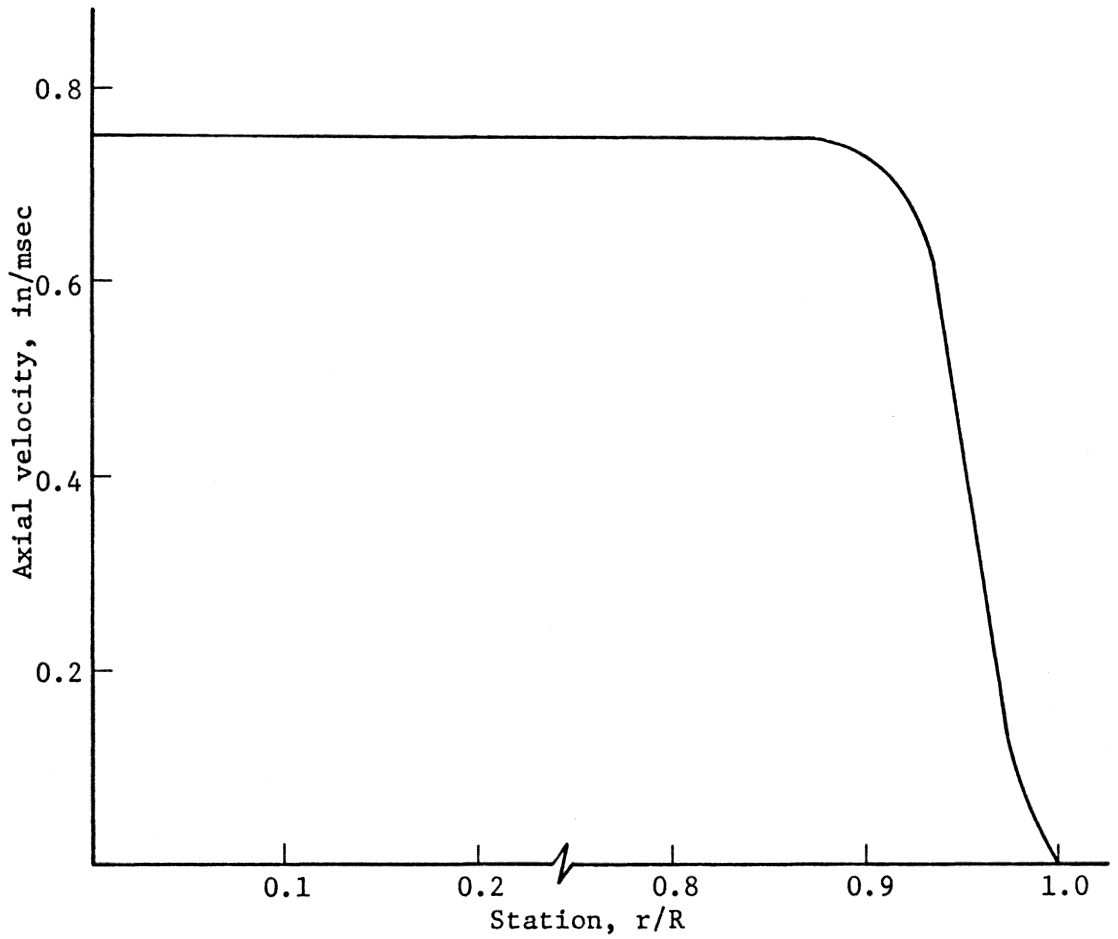

Figure 17. Axial velocity distribution at t = 28 microseconds.

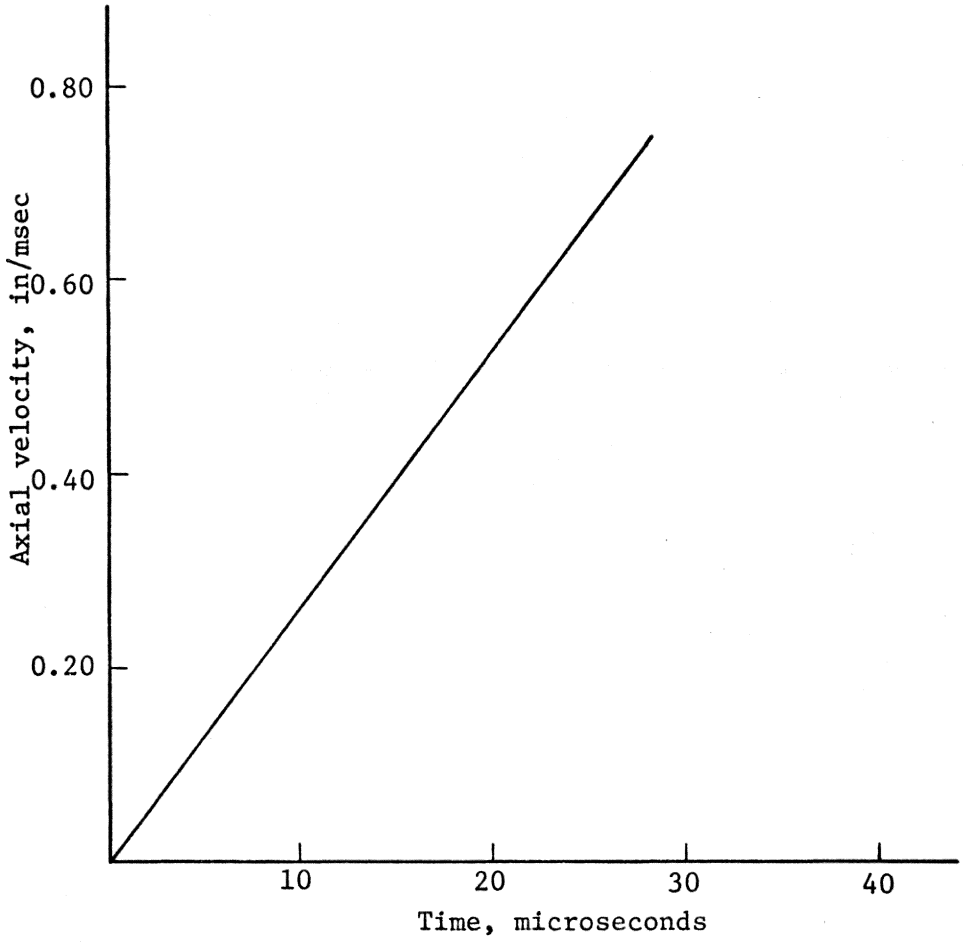

Figure 18. Axial velocity of center of the membrane as a function of time.

center and the inertia wave front moves upward with the same constant axial acceleration. After the inertia wave passes the point, the acceleration of that point is reduced by the vertical component of the meridional stress acting along the sloped portion of the membrane. The time history of the velocity of a typical point is shown in Figure 19.

Although it has not been analyzed numerically here, the phenomena occurring at the center of the membrane will remain the same during the plastic phase of the deformation. The center will continue to move upward with a constant acceleration until such time as it is reached by the inertia wave. After this time, the center will be decelerated until equilibrium is reached or, as is most likely, until the membrane ruptures.

Radial Velocity

In the analysis by Hudson [1], it was assumed that the stress state was such that the stress everywhere was equal to the yield stress. As Hudson's approach used the principles of work-energy and impulse-momentum, the elastic phase of deformation was not neglected completely as is reflected by his words: "Although the initial elastic effects occur very rapidly, they may result in a radial velocity distribution of significantly large order of magnitude." To include this elastic effect, Hudson assumed an initial velocity distribution that increases from zero at the center to a maximum at the boundary. The radial velocity distribution at the end of the elastic phase is shown in

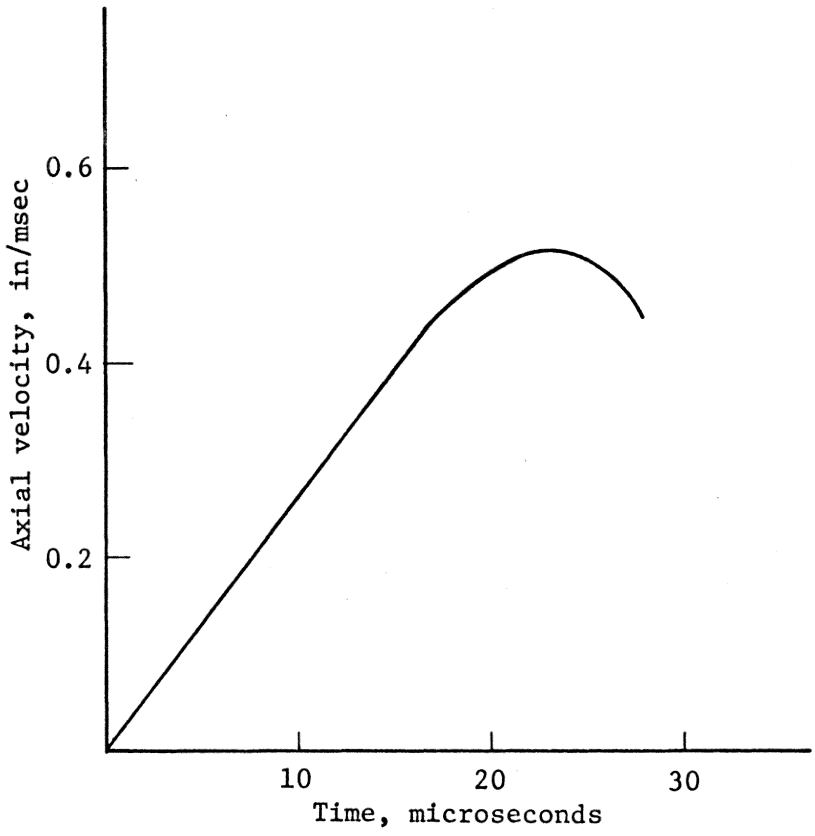

Figure 19. Axial velocity at r/R = 0.95 as a function of time.

Figure 20. The radial velocity increases from zero at the center to a maximum at a distance of about 90% of the radius. In the vicinity of the fixed boundary, however, a negative velocity gradient exists in order to satisfy the boundary condition of zero velocity at the fixed edge. The magnitude of the radial velocity component is as high as 20% of the corresponding axial velocity at some points. Thus, Hudson's assumptions are in good agreement with the numerical results from the complete equations of motion.

Effect of Pressure Magnitude on Yield Point

The preceding results show that for the membrane considered, an applied pressure of 33.3 psi resulted in an elastic phase of 28 microseconds duration. Yielding was observed to first occur near the fixed boundary, and a short time thereafter yielding had occurred throughout the membrane. In order to determine the effect of increased pressure on the position at which yielding first occurs, numerical results were obtained for an applied pressure of 66.6 psi with the membrane size and initial conditions unchanged.

Figure 21 gives the meridional stress distribution at several different times just after the leading strain wave front reaches the center of the membrane. The lower curve corresponding to t = 13 microseconds shows that the stress at the center of the membrane is 13,300 psi. The upper curve which corresponds to t = 14 microseconds reveals that in a time interval of only one microsecond, the stress at the center has increased to 20,500. Thus, the material at the center of

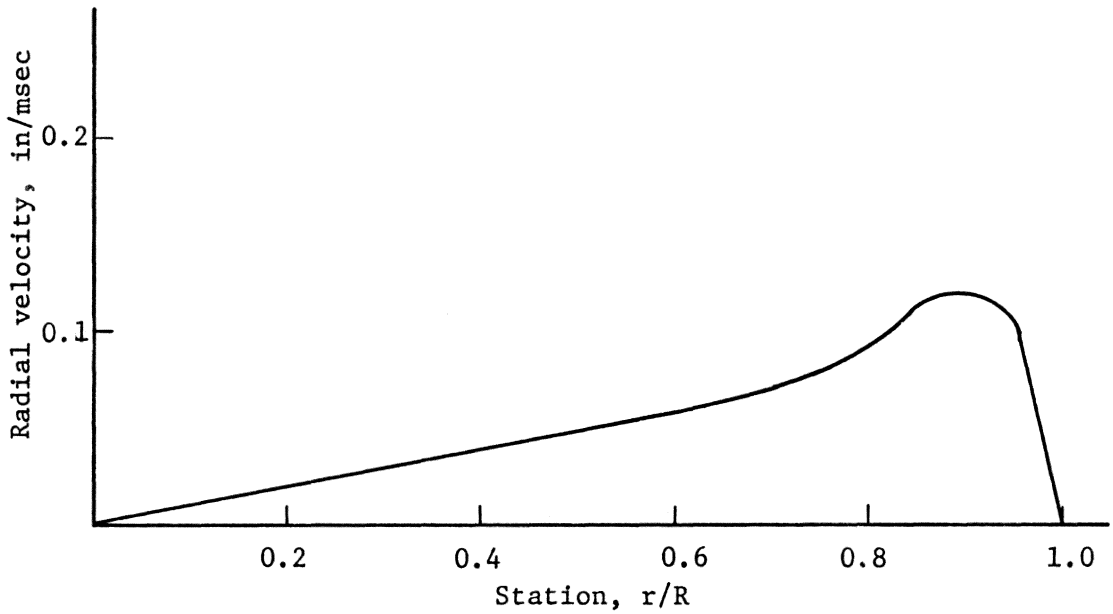

Figure 20. Radial velocity distribution at yield.

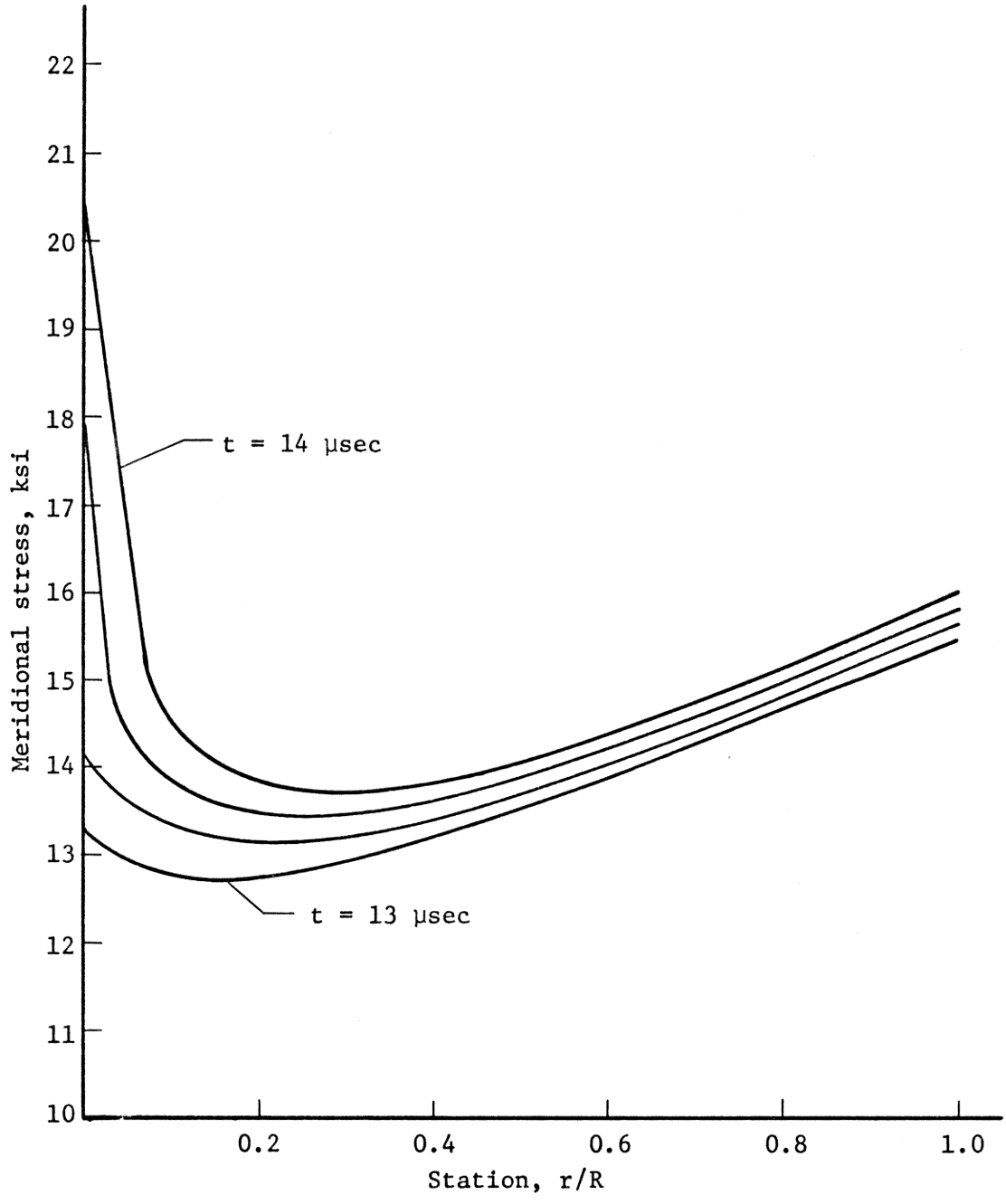

Figure 21. Meridional stress distribution at succeeding times for increased loading.

the membrane has yielded while the remainder of the membrane is still in the elastic state.

The results for the increased pressure are in contrast to the previous results where yielding was found to first occur near the fixed boundary. This phenomenon is accounted for by the fact that increasing the applied pressure also increases the jump in stress existing across the strain wave fronts. As the first and succeeding wave fronts reach the center of the membrane, they interact with wave fronts travelling diametrically opposite. The result is that the stress at the center increases very rapidly and exceeds the yield point before the reflecting waves have any appreciable effect on the outer portion of the membrane.

The result of increased pressure on yielding is twofold: (1) as would be expected, yielding occurs in a shorter time interval which reduces the total time of the elastic phase of the deformation; (2) the position at which yielding first occurs changes with pressure.

Axial Deflection

For the material considered, the deflection at the center of the membrane is small during the elastic phase of deformation. At the end of the elastic period the central deflection is only 0.03 inch for a six inch diameter membrane. In order to exhibit the effect of the inertia wave on the membrane, numerical results were also obtained for a hypothetical elastic material having an elastic modulus of 100,000 psi. The membrane diameter and thickness as well as the applied

pressure were unchanged. The profiles of the hypothetical membrane at various stages during the deformation are shown in Figure 22. The flat central portion ahead of the inertia wave front is apparent, and it is seen that the membrane becomes conical in shape as the wave front approaches the center. It must be pointed out that for this case the strain components are on the order of 5%, and it would be more appropriate to introduce logarithmic strain components.

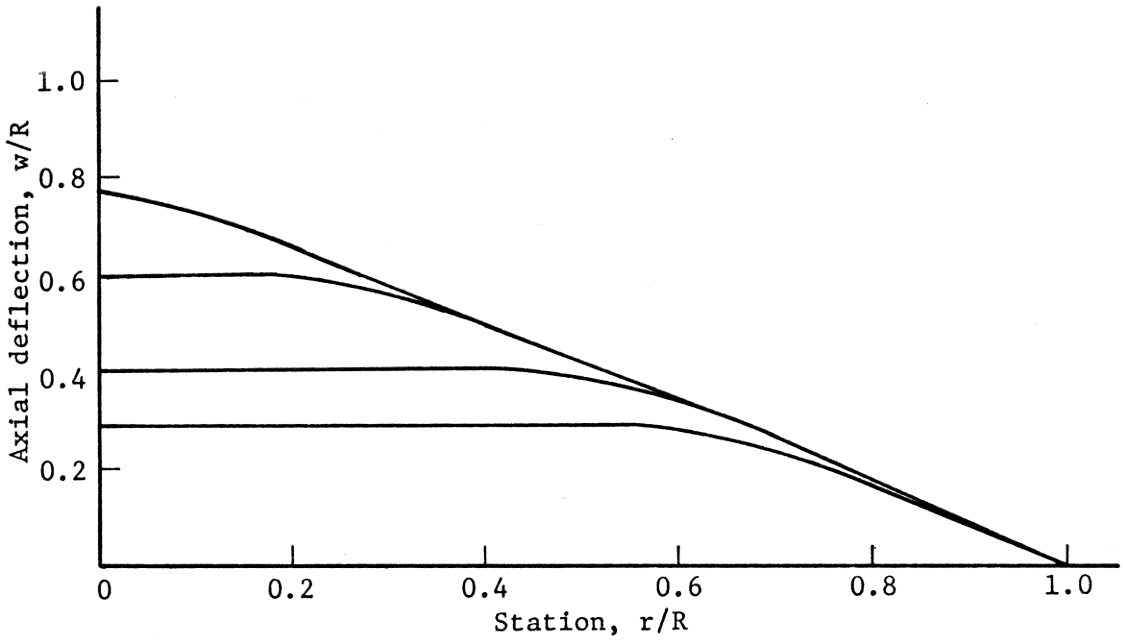

Figure 22. Successive membrane profiles for a hypothetical elastic material.

V. CONCLUDING REMARKS

Using the method of characteristics, a numerical solution has been obtained for the elastic deformation of a circular membrane subjected to an impulsive pressure loading. The total time for the elastic phase of the deformation was found to be less than 30 microseconds for the membrane and loading considered. The corresponding maximum elastic deflection is six times the initial thickness of the membrane. Although the deflections are small, both radial and axial velocities are found to be large enough in magnitude to merit taking them into account in extending the study to the plastic phase of deformation.

The inertia wave propagates inward from the fixed boundary as a discontinuity in the slope of the membrane. At the end of the elastic phase, the slope discontinuity is located 15% of the radius inward from the fixed boundary. Thus, the membrane profile is that of a flat, circular region connected to the fixed boundary by an outer region which is conical in shape. Both the propagation of the slope discontinuity and the membrane profile are in agreement with the experimental results obtained by Munday and Newitt [3], and the assumed mode of deformation of Hudson [1] and Frederick [2]. The membrane material in the flat region moves upward with a constant acceleration due to the pressure loading while the conical region is decelerated by forces resulting from the components of stress in the axial direction.

The velocity of the strain wave is such that the leading wave front propagates completely across the membrane and is reflected from the fixed boundary. For an applied pressure of 33.3 psi, yielding

occurs first near the fixed boundary, and the entire membrane then reaches yield in a very short time. Thus, the observed discontinuity in slope is not a plastic hinge of the type encountered when bending is taken into account; rather, it is simply an inertia effect. This observation is reinforced by the results for an applied pressure of 66.6 psi. These results show that yielding first occurs at the center of the membrane while the slope discontinuity has again propagated only a small distance inward from the boundary.

As shown in the analysis of the governing equations, the characteristics are functions of the strain components and were expected to be curved lines. However, the numerical results show that both inertia and strain waves propagate with essentially constant velocity during the elastic deformation. Thus, the characteristics are straight lines, and the variation due to changes in the magnitudes of the strain components is not significant in the elastic range. If the observation that the characteristics are linear is taken into account, it should be possible to simplify the equations of motion such that an approximate, closed-form solution can be obtained for the elastic deformation.

The general method of analysis presented is applicable to any finite constitutive equation; in particular, the method may be used to study the deformations corresponding to plastic constitutive equations. In modifying the numerical procedure to include plasticity, it would be necessary to include the appropriate yield criteria as a switching mechanism. When yielding occurs at a point, the program would be switched such that subsequent calculations are then performed using the

plastic constitutive equation. If, however, the previously mentioned approximate, closed-form solution can be obtained for the elastic deformation, the results may be used as input data for the plasticity computations. The complete numerical procedure for the elastic phase would not be required nor would the automatic switching based on the yield criteria. Thus, both programming effort and computation time would be significantly reduced. The latter approach will be used in seeking to extend the study to the domain of plastic material behavior.

Another area of interest is the deformation of membrane materials which exhibit anisotropic behavior. The analysis presented is directly applicable to anisotropic materials as long as the behavior is such that axial symmetry is preserved. A specific problem of interest is the study of a membrane having both radial and circumferential reinforcement. In this case the material behavior is orthotropic, and axial symmetry is maintained.

LIST OF REFERENCES

1. Hudson, G. E.: Theory of the Dynamic Plastic Deformation of a Thin Diaphragm. Journal of Applied Physics. Vol. 22, No. 1, January, 1951.

2. Frederick, D.: A Simplified Analysis of Circular Membranes Subjected to an Impulsive Loading Producing Large Plastic Deformations. Fourth Midwestern Conference on Solid Mechanics, 1959.

3. Munday, G.; and Newitt, D. M.: Philosophical Transactions of the Royal Society of London. Series A, Vol. 256, 1963.

4. Cristescu, N.: Dynamic Plasticity. North-Holland Publishing Company, 1967.

5. Kay, F. J.; and Whitehouse, G. D.: A Solution of the Plastic Deformation of Clamped Rectangular Membranes Subjected to Dynamic Loading. Pacific Symposium on Hydromechanically Loaded Shells, 1971.

6. Karunes, B.; and Onat, E. T.: Plastic-Wave Propagation Effects in Transverse Impact of Membranes. Journal of Applied Mechanics. Series E, Vol. 27, No. 1, March, 1960.

7. Chou, P. C.; and Perry, R. F.: The Classification of Partial Differential Equations in Structural Dynamics. AIAA Structural Dynamics and Aero-elasticity Specialist Conference. April, 1969.

8. Chou, P. C.; and Mortimer, R. W.: Solution of One-Dimensional Elastic Wave Problems by the Method of Characteristics. Journal of Applied Mechanics. Vol. 34, No. 3, 1967.

9. Frederick, D.; and Chang, T. S.: Continuum Mechanics. Allyn and Bacon, 1965.

10. Timoshenko, S.; and Young, D. F.: Elements of Strength of Materials. D. Van Nostrand, 1962.

11. Cristescu, N.; and Suliciu, I.: Rapid Motions of Circular Membranes. Revue Roumaine de Mathematics Pures et Applied. Vol. 12, No. 1, 1967.

APPENDIX A

Listing of Fortran programs used to obtain numerical results.

```
      IMPLICIT REAL*8 (A-H,O-Z)
      COMMON CTWO(2,201,2),ETA(2,201),ETAO(2,201),DOMEGN(2,201),DETADT(2
     1,201),E1(2,201),E2(2,201),E3(2,201),TAU(2,201),F2(2,201),H1(2,201)
     2,DETANO(2,201),SG1(2,201),SG2(2,201),OMEG(2,201),DOMEGT(2,201),CON
     3E5(202),CONE6(202),E,GNU,PZERO,TZERO,MAPROX,L,K,J
      READ (5,1) GNU,E,P,TZERO,J                                          1
    1 FORMAT(D8.3,F12.2,F9.2,F8.2,I4)                                     2
      READ(5,3) NX,NY,NU
    3 FORMAT(3I4)
      PZERO=P                                                             3
      INTRVL=J/2                                                          4
      WRITE(6,2) INTRVL                                                   5
    2 FORMAT(1H1,41HINITIAL NUMBER OF ETA ZERO INTERVALS IS  ,I4 )        6
C                                                                         7
C     DEFINE INITIAL CONDITIONS                                           8
C                                                                         9
      DO 5 K=1,J,1
      E1(1,K)= (1.D0-GNU)/E*TZERO                                        11
      E2(1,K)= E1(1,K)                                                   12
      E3(1,K)= -(2.D0*GNU/E)*TZERO                                       13
      SG1(1,K)=TZERO                                                     14
      SG2(1,K)= SG1(1,K)                                                 15
      CTWO(1,K,1)=((E+(1.D0-GNU)*TZERO)*(E-3.D0*GNU*TZERO-GNU**2.0*TZERO
     1)/(PZERO*(1.D0-GNU**2.0)*E))**0.5
      CTWO(1,K,2)=CTWO(1,K,1)
      W=K-1                                                              18
      Z=2*INTRVL                                                         18A
      ETA(1,K)=W/Z                                                       19
      ETAO(1,K)=ETA(1,K)                                                 20
      OMEG(1,K)= 0.D0                                                    21
      DETANO(1,K)= 1.D0+E1(1,K)                                          22
      DOMEGN(1,K)= 0.D0                                                  23
```

```
      DETADT(1,K)= 0.D0                                                    24
      DOMEGT(1,K)= 0.D0                                                    25
      TAU(1,K)= 0.D0                                                       26
      F2(1,K)=1.D0/(PZERO*(1.D0+E1(1,K)))*(SG1(1,K)*(1.D0+E2(1,K))*GNU/(232
     1GNU-1.D0)+(1.D0+E2(1,K))*(1.D0+E3(1,K))*GNU*E/(1.D0-GNU**2.0)+(1.0233
     20+E3(1,K))*SG1(1,K))
      CONE5(K+1)=((1.D0-2.D0*GNU/E*TZERO)*TZERO/PZERO)**0.5                29
    5 CONE6(K+1)=CONE5(K+1)
      E15=E1(1,1)                                                          31
      E16=E15                                                              32
      E25=E1(1,1)                                                          33
      E26=E25                                                              34
      E35=E3(1,1)                                                          35
      E36=E35                                                              36
      SG15=SG1(1,1)                                                        37
      SG16=SG15                                                            38
      SG25=SG15                                                            39
      SG26=SG15                                                            40
      DETAN5= 1.D0 + E15                                                   41
      DOMEG5= 0.D0                                                         42
      DETAN6= DETAN5                                                       43
      DOMEG6= DOMEG5                                                       44
C                                                                          45
C     INITIALIZE COUNTERS TO IDENTIFY FIRST OR SECOND APPROXIMATION        46
C                                                                          47
      L=1                                                                  48
      MAPROX=1                                                             49
      M=J-2
      TAU(2,1)=ETAO(1,2)/CTWO(1,2,1)
      DO 10 K=1,M,2
      IF(K.EQ.1) GO TO 9
      TAU(2,K)=(ETAO(1,K+1)-ETAO(1,K-1))/(CTWO(1,K+1,L)+CTWO(1,K-1,L))     61
```

```
    9 ETAO(2,K)=ETAO(1,K+1)-CTWO(1,K+1,L)*TAU(2,K)
      DOMEGT(2,K)=-(1.D0+E15)*(1.D0+E25)*TAU(2,K)
      DETADT(2,K)=DETADT(1,K+1)
      DOMEGN(2,K)=DOMEGN(1,K+1)
      DETANO(2,K)=DETANO(1,K+1)
      E1(2,K)=E1(1,K+1)
      E2(2,K)=E2(1,K+1)
      E3(2,K)=E3(1,K+1)
      SG1(2,K)=SG1(1,K+1)
      SG2(2,K)=SG2(1,K+1)
      F2(2,K)=F2(1,K+1)
      ETA(2,K)=ETAO(2,K)
      OMEG(2,K)=DOMEGT(2,K)/2.D0*TAU(2,K)
   10 CONTINUE                                                          110
      ETAO(2,J)=1.D0
      ETA(2,J)=1.D0
      DOMEGT(2,J)=0.D0
      DETADT(2,J)=0.D0
      OMEG(2,J)=0.D0
      E2(2,J)=(1.D0-GNU)/E*TZERO
      TAU(2,J)=(ETAO(2,J)-ETAO(1,J-1))/CTWO(1,J-1,L)
      DOMEGN(2,J)=((1.D0+E15)*(1.D0+E25)*TAU(2,J))/CONE5(J)
      DETANO(2,J)=DETANO(1,J-1)
      E1(2,J)=(DETANO(2,J)**2.0+DOMEGN(2,J)**2.0)**0.5-1.D0
      E3(2,J)=GNU/(GNU-1.D0)*(E1(2,J)+E2(2,J))
      SG1(2,J)=E/(1.D0-GNU**2.0)*(E1(2,J)+GNU*E2(2,J))
      SG2(2,J)=E/(1.D0-GNU**2.0)*(E2(2,J)+GNU*E1(2,J))
      F2(2,J)=1.D0/(PZERO*(1.D0+E1(2,J)))*(SG1(2,J)*(1.D0+E2(2,J))*GNU/(49
     1GNU-1.D0)+(1.D0+E2(2,J))*(1.D0+E3(2,J))*GNU*E/(1.D0-GNU**2.0)+(1.D50
     20+E3(2,J))*SG1(2,J))
C                                                                       111
C     PRINT RESULTS FROM FIRST ROW                                      112
```

```
C                                                                               113
      WRITE(6,99)                                                               114
   99 FORMAT(1HO,4X,4HETAO,13X,3HETA,14X,4HOMEG,14X,3HTAU,15X,2HE1,15X,2115
     1HE2,15X,2HE3//22X,3HSG1,15X,3HSG2,13X,6HDOMEGN,11X,6HDOMEGT,11X,6H116
     2DETADT,11X,6HDETANO)
      WRITE(6,100) (ETAO(2,K),ETA(2,K),OMEG(2,K),TAU(2,K),E1(2,K),E2(2,K118
     1),E3(2,K),SG1(2,K),SG2(2,K),DOMEGN(2,K),DOMEGT(2,K),DETADT(2,K),DE119
     2TANO(2,K),K=NX,J,NY)
      NO=2
      M=J-1
      N=2
      LX=NU
   83 DO 13 K=N,M,2
      IF(K.EQ.1) GO TO 42
      IF(K.EQ.J) GO TO 43
      CTWO(2,1,L)=(E/(1.DO-GNU**2.0)*(1.DO+E2(2,1))/PZERO*(GNU/(GNU-1.DO127
     1)*(2.DO*E1(2,1)+E2(1,2)+GNU*E2(1,2))+1.DO))**0.5                          128
      H1(NO,K+1)=((1.DO+E3(NO,K+1))*SG2(NO,K+1)*DETANO(NO,K+1)/PZERO+(1.156
     1DO+E1(NO,K+1))*(1.DO+E2(NO,K+1)-DETANO(NO,K+1))*F2(NO,K+1)-(1.DO+E157
     22(NO,K+1))*(1.DO+E3(NO,K+1))*SG1(NO,K+1) /PZERO)/ETAO(NO,K+1)             158
   82 CTWO(NO,K+1,L)=(E/(1.DO-GNU**2.0)*(1.DO+E2(NO,K+1))/PZERO*(GNU/(GN151
     1U-1.DO)*(2.DO*E1(NO,K+1)+E2(NO,K+1)+GNU*E2(NO,K+1))+1.DO))**0.5           152
   22 TAU(2,K)=(ETAO(NO,K+1)-ETAO(NO,K-1)+CTWO(NO,K-1,L)*TAU(NO,K-1)+CTW153
     1O(NO,K+1,L)*TAU(NO,K+1))/(CTWO(NO,K-1,L)+CTWO(NO,K+1,L))                  154
      ETAO(2,K)=ETAO(NO,K-1)+CTWO(NO,K-1,L)*(TAU(2,K)-TAU(NO,K-1))              155
   19 IF(MAPROX.EQ.2) GO TO 20                                                  164
      E1(2,K)=0.5DO*(E1(NO,K-1)+E1(NO,K+1))
      E2(2,K)=0.5DO*(E2(NO,K-1)+E2(NO,K+1))
      E3(2,K)=GNU/(GNU-1.DO)*(E1(2,K)+E2(2,K))                                  166
      CONE5(K)=((1.DO+E3(2,K))*E/(1.DO-GNU**2.0)*(E1(2,K)+GNU*E2(2,K))*(167
     11.DO+E2(2,K))/((1.DO+E1(2,K))*PZERO))**0.5                                168
      CONE6(K)=CONE5(K)
```

```
20 EONE=0.5D0*(E1(1,K)+E1(NO,K-1))                                    170
   ETWO=0.5D0*(E2(1,K)+E2(NO,K-1))                                    171
   CTWO(1,K,1)=(E/(1.D0-GNU**2.0)*(1.D0+ETWO)/PZERO*(GNU/(GNU-1.D0)*(172
  12.D0*EONE+ETWO+GNU*ETWO)+1.D0))**0.5                               173
   EONE=0.5D0*(E1(1,K)+E1(NO,K+1))                                    174
   ETWO=0.5D0*(E2(1,K)+E2(NO,K+1))                                    175
   CTWO(1,K,2)=(E/(1.D0-GNU**2.0)*(1.D0+ETWO)/PZERO*(GNU/(GNU-1.D0)*(176
  12*EONE+ETWO+GNU*ETWO)+1.D0))**0.5                                  177
   TAU5=(CONE5(K)*TAU(2,K)+CTWO(1,K,1)*TAU(1,K)+ETAO(1,K)-ETAO(2,K))/178
  1(CONE5(K)+CTWO(1,K,1))                                             179
   ETAO5=ETAO(1,K)-CTWO(1,K,1)*(TAU5-TAU(1,K))                        180
   TAU6=(CONE5(K)*TAU(2,K)+CTWO(1,K,2)*TAU(1,K)-(ETAO(1,K)-ETAO(2,K))181
  1)/(CONE5(K)+CTWO(1,K,2))
   ETAO6=ETAO(1,K)+CTWO(1,K,2)*(TAU6-TAU(1,K))                        183
   B10=(ETAO5-ETAO(1,K))/(ETAO(NO,K-1)-ETAO(1,K))                     184
   B11=(TAU5-TAU(1,K))/(TAU(NO,K-1)-TAU(1,K))                         185
   B12=(ETAO6-ETAO(1,K))/(ETAO(NO,K+1)-ETAO(1,K))                     186
   B13=(TAU6-TAU(1,K))/(TAU(NO,K+1)-TAU(1,K))                         187
   DETAN5=DETANO(1,K)+(DETANO(NO,K-1)-DETANO(1,K))*B10                188
   DOMEG5=DOMEGN(1,K)+(DOMEGN(NO,K-1)-DOMEGN(1,K))*B10                189
   DETAT5=DETADT(1,K)+(DETADT(NO,K-1)-DETADT(1,K))*B11                190
   DOMET5=DOMEGT(1,K)+(DOMEGT(NO,K-1)-DOMEGT(1,K))*B11                191
   DETAN6=DETANO(1,K)+(DETANO(NO,K+1)-DETANO(1,K))*B12                192
   DOMEG6=DOMEGN(1,K)+(DOMEGN(NO,K+1)-DOMEGN(1,K))*B12                193
   DETAT6=DETADT(1,K)+(DETADT(NO,K+1)-DETADT(1,K))*B13                194
   DOMET6=DOMEGT(1,K)+(DOMEGT(NO,K+1)-DOMEGT(1,K))*B13                195
   E15=E1(1,K)+(E1(NO,K-1)-E1(1,K))*B10                               196
   E25=E2(1,K)+(E2(NO,K-1)-E2(1,K))*B10
   E35=GNU/(GNU-1.D0)*(E15+E25)                                       199
   E16=E1(1,K)+(E1(NO,K+1)-E1(1,K))*B12                               200
   E26=E2(1,K)+(E2(NO,K+1)-E2(1,K))*B12                               201
   E36=GNU/(GNU-1.D0)*(E16+E26)                                       202
```

```
      SG25=E/(1.D0-GNU**2.0)*(E25+GNU*E15)
      SG26=E/(1.D0-GNU**2.0)*(E26+GNU*E16)
      C15=(1.D0+E15)*((1.D0+E35)*SG25*DOMEG5/(ETA05*PZERO)-(1.D0+E15)*(1
     1.D0+E25))
      C16=(1.D0+E16)*((1.D0+E36)*SG26*DOMEG6/(ETA06*PZERO)-(1.D0+E16)*(1
     1.D0+E26))
      DTAU5=TAU(2,K)-TAU5
      DTAU6=TAU(2,K)-TAU6
      IF(K.EQ.2) GO TO 300
      C21=(1.D0+E1(NO,K-1))*H1(NO,K-1)
      GO TO 301
  300 C21=0.D0
  301 C23=(1.D0+E1(NO,K+1))*H1(NO,K+1)
      DTAU1=TAU(2,K)-TAU(NO,K-1)
      DTAU3=TAU(2,K)-TAU(NO,K+1)
      A1=DOMEGN(NO,K-1)
      B1=DETANO(NO,K-1)
      D1=DOMEGT(NO,K-1)
      H2=DETADT(NO,K-1)
      A3=DOMEGN(NO,K+1)
      B3=DETANO(NO,K+1)
      D3=DOMEGT(NO,K+1)
      H3=DETADT(NO,K+1)
      A5=DOMEG5
      B5=DETAN5
      D5=DOMET5
      E5=DETAT5
      A6=DOMEG6
      B6=DETAN6
      D6=DOMET6
      E6=DETAT6
      G1=(CTWO(NO,K-1,L)-CONE5(K))/(CONE6(K)+CONE5(K))
```

```
 G2=CTWO(NO,K-1,L)+A1/B1*G1*(CONE6(K)*A6/B6+CONE5(K)*A5/B5)+CONE5(K
1)*A1/B1*A5/B5
 G3=A3/B3*A5/B5
 G4=A3/B3*(CTWO(NO,K+1,L)+CONE5(K))/(CONE6(K)+CONE5(K))
 G5=1.D0+G3+G4*(A6/B6-A5/B5)
 G6=CTWO(NO,K+1,L)-G3*CONE5(K)+G4*(CONE6(K)*A6/B6+CONE5(K)*A5/B5)
 G7=G5+G6/G2*(1.D0-A1/B1*G1*(A6/B6-A5/B5)+A1/B1*A5/B5)
 G8=A5/B5*E5-A6/B6*E6
 G9=C16/B6*DTAU6-C15/B5*DTAU5
 STAR=A3/B3*(C15/B5*DTAU5+D5-A5/B5*E5)
 DETADT(2,K)=1.D0/G7*(CTWO(NO,K+1,L)/B3*(B3**2.0+A3*A3   )+H3+A3/B3*
1D3-C23/B3*DTAU3-G4*(G8+G9+D6-D5)-G6/G2*(C21/B1*DTAU1+CTWO(NO,K-1,L
2)*B1-H2+A1/B1*(CTWO(NO,K-1,L)*A1-D1-G1*G8-G1*G9-G1*(D6-D5)+C15/B5*
3DTAU5+D5-A5/B5*E5)))-STAR/G7
 IF(DETADT(2,K).LT.0.D0) DETADT(2,K)=0.D0
 DETANO(2,K)=1.D0/G2*(C21/B1*DTAU1+CTWO(NO,K-1,L)*B1-H2+DETADT(2,K)
1+A1/B1*(CTWO(NO,K-1,L)*A1-D1-G1*(A6/B6-A5/B5)*DETADT(2,K)-G1*G8-G1
2*G9-G1*(D6-D5)+C15/B5*DTAU5+D5+A5/B5*DETADT(2,K)-A5/B5*E5))
 DOMEGN(2,K)=1.D0/(CONE6(K)+CONE5(K))*(DETANO(2,K)*(CONE6(K)*A6/B6+
1CONE5(K)*A5/B5)+DETADT(2,K)*(A6/B6-A5/B5)+G8+G9-D5+D6)
 DOMEGT(2,K)=C15/B5*DTAU5+D5+CONE5(K)*DOMEGN(2,K)-CONE5(K)*A5/B5*DE
1TANO(2,K)+A5/B5*(DETADT(2,K)-E5)
 E1(2,K)=(DETANO(2,K)**2.0+DOMEGN(2,K)*DOMEGN(2,K))**0.5-1.D0
 OMEG6=OMEG(1,K)+(OMEG(NO,K+1)-OMEG(1,K))*B13
 ETA(2,K)=ETA(NO,K-1)+((DETANO(NO,K-1)+DETANO(2,K))/2.D0-(1.D0-GNU)
1/E*TZERO)*(ETAO(2,K)-ETAO(NO,K-1))+(DETADT(NO,K-1)+DETADT(2,K))/2.
2D0*(TAU(2,K)-TAU(NO,K-1))
 OMEG(2,K)=OMEG6+0.5D0*(DOMEG6+DOMEGN(2,K))*(ETAO(2,K)-ETAO6)+0.5D0
1*(DOMET6+DOMEGT(2,K))*(TAU(2,K)-TAU6)
 E2(2,K)=ETA(2,K)/ETAO(2,K)*(1.D0+(1.D0-GNU)/E*TZERO)-1.D0
 E3(2,K)=GNU/(GNU-1.D0)*(E1(2,K)+E2(2,K))                              229
 SG1(2,K)=E/(1.D0-GNU**2.0)*(E1(2,K)+GNU*E2(2,K))                      230
```

```
      SG2(2,K)=E/(1.D0-GNU**2.0)*(E2(2,K)+GNU*E1(2,K))                    231
      F2(2,K)=1.D0/(PZERO*(1.D0+E1(2,K)))*(SG1(2,K)*(1.D0+E2(2,K))*GNU/(232
     1GNU-1.D0)+(1.D0+E2(2,K))*(1.D0+E3(2,K))*GNU*E/(1.D0-GNU**2.0)+(1.0233
     20+E3(2,K))*SG1(2,K))
      IF(MAPROX.EQ.2) GO TO 23                                           234
      L=2                                                                235
      MAPROX=2                                                           236
      EONE=0.5D0*(E1(NO,K-1)+E1(2,K))                                    237
      ETWO=0.5D0*(E2(NO,K-1)+E2(2,K))                                    238
      CTWO(NO,K-1,L)=(E/(1.D0-GNU**2.0)*(1.D0+ETWO)/PZERO*(GNU/(GNU-1.D0239
     1)*(2.D0*EONE+ETWO+GNU*ETWO)+1.D0))**0.5                           240
      EONE=0.5D0*(E1(NO,K+1)+E1(2,K))                                    241
      ETWO=0.5D0*(E2(NO,K+1)+E2(2,K))                                    242
      CTWO(NO,K+1,L)=(E/(1.D0-GNU**2.0)*(1.D0+ETWO)/PZERO*(GNU/(GNU-1.D0243
     1)*(2.D0*EONE+ETWO+GNU*ETWO)+1.D0))**0.5                           244
      CONE5(K)=((1.D0+E2(2,K))*(1.D0+E3(2,K))*SG1(2,K) /((1.D0+E1(2,K))*245
     1PZERO))**0.5                                                      246
      CONE6(K)=CONE5(K)
      GO TO 22                                                           249
   23 L=1                                                                250
      MAPROX=1                                                           251
      GO TO 13                                                           252
C                                                                        253
C     CALL SUBROUTINE FOR RIGHT BOUNDARY                                 254
C                                                                        255
   43 CALL RBOUND
      GO TO 13
C     CALL SUBROUTINE FOR LEFT BOUNDARY                                  143
C                                                                        144
   42 CALL BOUNDL
   13 CONTINUE
      WRITE(6,100) (ETAO(2,K),ETA(2,K),OMEG(2,K),TAU(2,K),E1(2,K),E2(2,K259
```

```
   1),E3(2,K),SG1(2,K),SG2(2,K),DOMEGN(2,K),DOMEGT(2,K),DETADT(2,K),DE
   2TANO(2,K),K=LX,M,NY)
100 FORMAT(1HO,(7(F12.7,5X)/17X,2(F12.4,5X),4(F12.7,5X)/))
    IF(N.EQ.2) GO TO 81
    NO=2
    M=J-1
    N=2
    LX=NU
    GO TO 83
 81 IF(SG1(2,J).GT.40000.0) GO TO 86
    NO=1
    N=1
    M=J
    LX=NX
    CALLREDEF
    GO TO 83
 86 CONTINUE
    STOP                                                          267
    END                                                           268
```

```
      SUBROUTINE BOUNDL
      IMPLICIT REAL*8 (A-H,O-Z)
      COMMON CTWO(2,201,2),ETA(2,201),ETAO(2,201),DOMEGN(2,201),DETADT(2
     1,201),E1(2,201),E2(2,201),E3(2,201),TAU(2,201),F2(2,201),H1(2,201)
     2,DETANO(2,201),SG1(2,201),SG2(2,201),OMEG(2,201),DOMEGT(2,201),CON
     3E5(202),CONE6(202),E,GNU,PZERO,TZERO,MAPROX,L,K,J
      ETA(2,1)=0.D0                                                      4
      ETAO(2,1)=0.D0                                                     5
      DOMEGN(2,1)=0.D0                                                   6
      DETADT(2,1)=0.D0                                                   8
      CTWO(1,2,L)=((E/(1.D0-GNU**2.0)*(1.D0+E2(1,2))/PZERO)*((GNU/(GNU-19
     1.D0)*(2.D0*E1(1,2)+E2(1,2)+GNU*E2(1,2))+1.D0)))**0.5
   11 TAU(2,1)=(ETAO(1,2)-ETAO(2,1)+CTWO(1,2,L)*TAU(1,2))/CTWO(1,2,L)    11
      H1(1,2)=((1.D0+E3(1,2))*SG2(1,2)*DETANO(1,2)/PZERO+(1.D0+E1(1,2))*12
     1(1.D0+E2(1,2)-DETANO(1,2))*F2(1,2)-(1.D0+E2(1,2))*(1.D0+E3(1,2))*S13
     2G1(1,2)/PZERO)/ETAO(1,2)                                          14
      IF(MAPROX.EQ.2) GO TO 50                                          17
      CONE6(1)=((1.D0+E2(1,2))*(1.D0+E3(1,2))*SG1(1,2)/((1.D0+E1(1,2))*P
     1ZERO))**0.5
   50 TAU6=(CONE6(1)*TAU(2,1)+CTWO(1,1,2)*TAU(1,1))/(CONE6(1)+CTWO(1,1,221
     1))                                                                22
      ETAO6=CONE6(1)*(TAU(2,1)-TAU6)                                    23
      DETAN6=DETANO(1,1)+(DETANO(1,2)-DETANO(1,1))*(ETAO6-ETAO(1,1))/(ET24
     1AO(1,2)-ETAO(1,1))                                                25
      DOMEG6=DOMEGN(1,1)+(DOMEGN(1,2)-DOMEGN(1,1))*(ETAO6-ETAO(1,1))/(ET26
     1AO(1,2)-ETAO(1,1))                                                27
      DETAT6=DETADT(1,1)+(DETADT(1,2)-DETADT(1,1))*(TAU6-TAU(1,1))/(TAU(28
     11,2)-TAU(1,1))                                                    29
      DOMET6=DOMEGT(1,1)+(DOMEGT(1,2)-DOMEGT(1,1))*(TAU6-TAU(1,1))/(TAU(30
     11,2)-TAU(1,1))                                                    31
      E16=E1(1,1)+(E1(1,2)-E1(1,1))*(ETAO6-ETAO(1,1))/(ETAO(1,2)-ETAO(1,32
     11))                                                               33
```

```
 E26=E2(1,1)+(E2(1,2)-E2(1,1))*(ETAO6-ETAO(1,1))/(ETAO(1,2)-ETAO(1,36
11))                                                                    37
 E36=GNU/(GNU-1.D0)*(E16+E26)                                           38
 SG26=E/(1.D0-GNU**2.0)*(E26+GNU*E16)
 C16=(1.D0+E16)*((1.D0+E36)*SG26*DOMEG6/(ETAO6*PZERO)-(1.D0+E16)*(1
1.D0+E26))
 DTAU6=TAU(2,1)-TAU6
 C23=(1.D0+E1(1,2))*H1(1,2)
 DTAU3=TAU(2,1)-TAU(1,2)
 G10=CTWO(1,2,L)*DETANO(1,2)+CONE6(1)*DOMEG6*DOMEGN(1,2)/DETAN6
 DETANO(2,1)=1.D0/G10*(CTWO(1,2,L)*(1.D0+E1(1,2))**2.0+DETANO(1,2)*
1DETADT(1,2)+DOMEGN(1,2)*DOMEGT(1,2)-C23*DTAU3-DOMEGN(2,1)/DETAN6*(
2C16*DTAU6+DETAN6*DOMET6-DOMEG6*DETAT6))
 DOMEGT(2,1)=1.D0/DETAN6*(C16*DTAU6+DETAN6*DOMET6-DOMEG6*DETAT6+CON
1E6(K)*DOMEG6*DETANO(2,1))
 E1(2,1)=DETANO(2,1)-1.D0
 OMEG6=OMEG(1,1)+(OMEG(1,2)-OMEG(1,1))*DTAU6/(TAU(1,2)-TAU(1,1))
 OMEG(2,1)=OMEG6+0.5D0*(DOMET6+DOMEGT(2,1))*DTAU6-0.5D0*DOMEG6*ETAO
16
 E2(2,1)=E1(2,1)                                                        49
 E3(2,1)=GNU/(GNU-1.D0)*(E1(2,1)+E2(2,1))                               50
 SG1(2,1)=E/(1.D0-GNU**2.0)*(E1(2,1)+GNU*E2(2,1))                       51
 SG2(2,1)=E/(1.D0-GNU**2.0)*(E2(2,1)+GNU*E1(2,1))                       52
 F2(2,1)=1.D0/(PZERO*(1.D0+E1(2,1)))*(SG1(2,1)*(1.D0+E2(2,1))*GNU/(53
1GNU-1.D0)+(1.D0+E2(2,1))*(1.D0+E3(2,1))*GNU*E/(1.D0-GNU**2.0)+(1.D54
20+E3(2,1))*SG1(2,1))                                                   55
 IF(MAPROX.EQ.2) GO TO 12                                               58
 L=2                                                                    59
 MAPROX=2                                                               60
 EONE=0.5D0*(E1(2,1)+E1(1,2))                                           61
 ETWO=0.5D0*(E2(2,1)+E2(1,2))                                           62
 CTWO(1,2,L)=((E/(1.D0-GNU**2.0))*(1.D0+ETWO)/PZERO*((GNU/(GNU-1.D063
```

```
     1))*(2.D0*EONE+ETWO+GNU*ETWO)+1.D0))**0.5                                  64
      CONE6(1)=((1.D0+E2(2,1))*(1.D0+E3(2,1))*SG1(2,1)/((1.D0+E1(2,1))*P65
     1ZERO))**0.5                                                               66
      GO TO 11                                                                  67
   12 L=1                                                                       68
      MAPROX=1                                                                  69
      RETURN                                                                    70
      END                                                                       71
```

```
      SUBROUTINE RBOUND
      IMPLICIT REAL*8 (A-H,O-Z)
      COMMON CTWO(2,201,2),ETA(2,201),ETAO(2,201),DOMEGN(2,201),DETADT(2
     1,201),E1(2,201),E2(2,201),E3(2,201),TAU(2,201),F2(2,201),H1(2,201)
     2,DETANO(2,201),SG1(2,201),SG2(2,201),OMEG(2,201),DOMEGT(2,201),CON
     3E5(202),CONE6(202),E,GNU,PZERO,TZERO,MAPROX,L,K,J
      ETA(2,K)=1.D0
      ETAO(2,K)=1.D0
      OMEG(2,K)=0.D0
      DOMEGT(2,K)=0.D0
      DETADT(2,K)=0.D0
   18 TAU(2,K)=TAU(1,K-1)+(ETAO(2,K)-ETAO(1,K-1))/CTWO(1,K-1,L)          11
      IF(MAPROX.EQ.2) GO TO 51
      CONE5(K)=((1.D0+E2(1,K-1))*(1.D0+E3(1,K-1))*SG1(1,K-1) /((1.D0+E1(15
     11,K-1))*PZERO))**0.5
   51 TAU5=(CONE5(K)*TAU(2,K)+CTWO(1,K,2)*TAU(1,K))/(CONE5(K)+CTWO(1,K,218
     1))
      ETAO5=ETAO(1,K)-CTWO(1,K,2)*(TAU5-TAU(1,K))
      DETAN5=DETANO(1,K)+(DETANO(1,K-1)-DETANO(1,K))*(ETAO5-ETAO(1,K))/(21
     1ETAO(1,K-1)-ETAO(1,K))
      DOMEG5=DOMEGN(1,K)+(DOMEGN(1,K-1)-DOMEGN(1,K))*(ETAO5-ETAO(1,K))/(23
     1ETAO(1,K-1)-ETAO(1,K))
      E15=E1(1,K)+(E1(1,K-1)-E1(1,K))*(ETAO5-ETAO(1,K))/(ETAO(1,K-1)-ETA25
     10(1,K))
      E25=E2(1,K)+(E2(1,K-1)-E2(1,K))*(ETAO5-ETAO(1,K))/(ETAO(1,K-1)-ETA27
     10(1,K))
      E35=GNU/(GNU-1.D0)*(E15+E25)
      DETAT5=DETADT(1,K)+(DETADT(1,K-1)-DETADT(1,K))*(TAU5-TAU(1,K))/(TA37
     1U(1,K-1)-TAU(1,K))
      DOMET5=DOMEGT(1,K)+(DOMEGT(1,K-1)-DOMEGT(1,K))*(TAU5-TAU(1,K))/(TA39
     1U(1,K-1)-TAU(1,K))
      SG25=E/(1.D0-GNU**2.0)*(E25+GNU*E15)
```

```
      C5=(1.D0+E15)*((1.D0+E35)*SG25*DOMEG5/(ETA05*PZERO)-(1.D0+E15)*(1.
     1D0+E25))
      A=(1.D0+E1(1,K-1))*H1(1,K-1)
      DETANO(2,K)=1.D0/(CONE5(K)*CTWO(1,K-1,L)*(DETANO(1,K-1)*DETAN5+DOM
     1EGN(1,K-1)*DOMEG5))*(CTWO(1,K-1,L)*DOMEGN(1,K-1)*(DETAN5*DOMET5+C5
     2*(TAU(2,K)-TAU5)-DOMEG5*DETAT5)+CONE5(K)*DETAN5*(CTWO(1,K-1,L)*DET
     3ANO(1,K-1)**2.0+CTWO(1,K-1,L)*DOMEGN(1,K-1)**2.0-DETANO(1,K-1)*DET
     4ADT(1,K-1)-DOMEGN(1,K-1)*DOMEGT(1,K-1)+A*(TAU(2,K)-TAU(1,K-1))))
      DOMEGN(2,K)=DOMEG5*(DETANO(2,K)/DETAN5+DETAT5/(CONE5(K)*DETAN5))-D
     1OMET5/CONE5(K)-(1.D0+E15)/(CONE5(K)*DETAN5)*((1.D0+E35)*SG25*DOMEG
     25/(ETA05*PZERO)-(1.D0+E15)*(1.D0+E25))*(TAU(2,K)-TAU5)
      E1(2,K)=(DOMEGN(2,K)**2.0+DETANO(2,K)**2.0)**0.5-1.D0
      E2(2,K)=(1.D0-GNU)/E*TZERO
      E3(2,K)=GNU/(GNU-1.D0)*(E1(2,K)+E2(2,K))
      SG1(2,K)=E/(1.D0-GNU**2.0)*(E1(2,K)+GNU*E2(2,K))
      SG2(2,K)=E/(1.D0-GNU**2.0)*(E2(2,K)+GNU*E1(2,K))
      F2(2,K)=1.D0/(PZERO*(1.D0+E1(2,K)))*(SG1(2,K)*(1.D0+E2(2,K))*GNU/(49
     1GNU-1.D0)+(1.D0+E2(2,K))*(1.D0+E3(2,K))*GNU*E/(1.D0-GNU**2.0)+(1.D50
     20+E3(2,K))*SG1(2,K))
      IF(MAPROX.EQ.2) GO TO 12
      L=2
      MAPROX=2
      EONE=0.5D0*(E1(1,K-1)+E1(2,K))
      ETWO=0.5D0*(E2(1,K-1)+E2(2,K))
      CTWO(1,K-1,L)= (E/(1.D0-GNU**2.0)*(1.D0+ETWO)/PZERO*((GNU/(GNU-1.D58
     10))*(2.D0*EONE+ETWO+GNU*ETWO)+1.D0))**0.5
      CONE5(K)=((1.D0+E2(2,K))*(1.D0+E3(2,K))*SG1(2,K)/((1.D0+E1(2,K))*P60
     1ZERO))**0.5
      GO TO 18
   12 L=1
      MAPROX=1
      RETURN
```

```
      SUBROUTINE REDEF
      IMPLICIT REAL*8 (A-H,O-Z)
      COMMON CTWO(2,201,2),ETA(2,201),ETAO(2,201),DOMEGN(2,201),DETADT(2
     1,201),E1(2,201),E2(2,201),E3(2,201),TAU(2,201),F2(2,201),H1(2,201)
     2,DETANO(2,201),SG1(2,201),SG2(2,201),OMEG(2,201),DOMEGT(2,201),CON
     3E5(202),CONE6(202),E,GNU,PZERO,TZERO,MAPROX,L,K,J
      CTWO(1,1,2)=CTWO(2,1,2)
      DO 90 K=1,J,1                                                     5
      E1(1,K)=E1(2,K)                                                   7
      E2(1,K)=E2(2,K)                                                   8
      E3(1,K)=E3(2,K)
      SG1(1,K)=SG1(2,K)                                                 10
      SG2(1,K)=SG2(2,K)                                                 11
      F2(1,K)=F2(2,K)                                                   12
      DETANO(1,K)=DETANO(2,K)                                           13
      DOMEGN(1,K)=DOMEGN(2,K)                                           14
      DETADT(1,K)=DETADT(2,K)                                           15
      DOMEGT(1,K)=DOMEGT(2,K)                                           16
      TAU(1,K)=TAU(2,K)                                                 18
      ETA(1,K)=ETA(2,K)                                                 19
      OMEG(1,K)=OMEG(2,K)                                               20
   90 ETAO(1,K)=ETAO(2,K)                                               21
      RETURN                                                            23
      END                                                               24
```

The vita has been removed from the scanned document

WAVE PROPAGATION IN A CIRCULAR MEMBRANE SUBJECTED TO AN IMPULSIVELY APPLIED PRESSURE LOAD

by

David Vernon Hutton

(ABSTRACT)

The elastic deformation of a circular membrane subjected to an impulsively applied pressure of constant magnitude is investigated. The membrane is assumed to be clamped at the periphery after being subjected to a small radial extension. The differential equations of motion are derived and classified as completely hyperbolic. Results are obtained using the method of characteristics and the technique of numerical integration along the characteristic lines.

Both strain waves and inertia waves propagate through the membrane as the deformation takes place. The numerical results show that while the membrane material is in the elastic range, the two types of waves propagate with constant, but unequal, velocities. It is pointed out that the phenomenon of constant wave velocities could possibly be used to simplify the equations of motion and obtain an approximate, closed form solution applicable to the elastic range.

Although only the elastic case is considered, the analysis presented is applicable to material behavior obeying any finite constitutive relation. In particular, extension of the procedure to the study of plastic deformation is discussed.